

1 **The Impact of Hurricane Disturbances on a Tropical Forest:**
2 **Implementing a Palm Plant Functional Type and Hurricane**
3 **Disturbance Module in ED2-HuDi V1.0**

4 Jiaying Zhang¹, Rafael L. Bras¹, Marcos Longo^{2,3}, Tamara Heartsill Scalley⁴

5 ¹School of Civil and Environmental Engineering, Georgia Institute of Technology, Atlanta, GA, United States

6 ²Jet Propulsion Laboratory, California Institute of Technology, Pasadena, CA, United States

7 ³Climate and Ecosystem Sciences Division, Lawrence Berkeley National Laboratory, Berkeley, CA, United States

8 ⁴USDA Forest Service, International Institute of Tropical Forestry, Río Piedras, PR, United States.

9 *Correspondence to:* Jiaying Zhang (jiaying.zhang@gatech.edu); Rafael L. Bras (rlbras@gatech.edu)

10

11 **Abstract**

12 Hurricanes commonly disturb and damage tropical forests. ~~It is predicted that changes in climate will result in changes~~
13 ~~in hurricane frequency and intensity. Hurricane frequency and intensity are predicted to change under the changing~~
14 ~~climate. The short-term impacts of hurricane disturbances to tropical forests have been widely studied, but the long-~~
15 ~~term impacts are rarely investigated.~~ Modeling is ~~critical to~~ ~~needed to~~ investigate the potential response of forests to
16 future disturbances, ~~particularly if the nature of the disturbances is changing with climate.~~ Unfortunately, existing
17 models of forests dynamics are not presently able to account for hurricane disturbances. ~~Therefore, W~~we implement
18 the Hurricane Disturbance in the Ecosystem Demography model (ED2) (ED2-HuDi). The hurricane disturbance
19 includes hurricane-induced immediate mortality and subsequent recovery modules. The parameterizations are based
20 on observations at the Bisley Experimental Watersheds (BEW) in the Luquillo Experimental Forest in Puerto Rico.
21 We add one new plant functional type (PFT) to the model—Palm, as palms cannot be categorized into one of the
22 current existing PFTs and are known to be an abundant component of tropical forests worldwide. The model is
23 calibrated with observations at BEW using the generalized likelihood uncertainty estimates (GLUE) approach. The
24 optimal simulation obtained from GLUE has a mean relative error of -21%, -12%, and -15% for stem density, basal
25 area, and aboveground biomass, respectively. The optimal simulation also agrees well with the observation in terms
26 of PFT composition (+1%, -8%, -2%, and +9% differences in the percentages of Early, Mid, Late, and Palm PFTs,
27 respectively) and size structure of the forest (+0.8% differences in the percentage of large stems). Lastly, using the
28 optimal parameter set, we study the impact of forest initial condition on the recovery of the forest from a single
29 hurricane disturbance. The results indicate that, compared to a no-hurricane scenario, a single hurricane disturbance
30 has little impact on forest structure (+1% change in the percentage of large stems) and composition (< 1% change in
31 the percentage of each of the four PFTs) but leads to 5% higher aboveground biomass after 80 years of succession.
32 The assumption of a less severe hurricane disturbance leads to a 4% increase in aboveground biomass.

33 **1 Introduction**

34 Hurricanes are an important disturbance agent in tropical forests. They damage individual trees and reduce
35 aboveground biomass (Zimmerman et al. 1994; Uriarte et al. 2019; Rutledge et al. 2021; Leitold et al. 2021; ~~Zhang et~~
36 ~~al. in revision~~). ~~For example, hurricane Hugo in 1989 uprooted and snapped 20% of the trees at El Verde in the~~
37 ~~Luquillo Experimental Forest (LEF), Puerto Rico (Walker 1991; Walker et al. 1992; Zimmerman et al. 1994) and~~
38 ~~reduced the aboveground biomass by 50% at Bisley in the LEF (Scatena et al. 1993; Heartsill Scalley et al. 2010).~~
39 ~~Hurricane Katrina in 2005 damaged about 320 million large trees on U.S. Gulf Coast forests, and the damaged trees~~
40 ~~are equivalent to 50-140% of the net annual U.S. carbon sink (Chambers et al. 2007).~~ In the long term, ~~they the~~
41 ~~recovery from those damages will~~ alter forest species composition and structure (Royo et al. 2011; Heartsill Scalley
42 2017; ~~Zhang et al. in revision~~).

43 Hurricane-induced mortality varies with many factors, including hurricane severity (Parker et al. 2018),
44 environmental conditions (Uriarte et al. 2019; Hall et al. 2020), ~~forest exposure to hurricane winds (Boose et al. 1994;~~
45 ~~Boose et al. 2004),~~ forest structure (Zhang et al. ~~in revision~~2022b), and traits and size of individual trees (Curran et

46 al. 2008; Lewis and Bannar-Martin 2011). Trees with a larger diameter have been found to be more resistant to wind
47 forces but more likely to suffer broken branches (Lewis and Bannar-Martin 2011). Species with higher wood density
48 tend to suffer less from hurricane disturbances (Zimmerman et al. 1994; Curran et al. 2008). Hurricanes with heavier
49 rainfall and stronger wind generally lead to higher mortality (Uriarte et al. 2019; Hall et al. 2020); and forests that are
50 more exposed to strong winds tend to have higher mortality (Uriarte et al. 2019). However, forests with a more wind-
51 resistant structure and composition experience lower mortality even during a stronger hurricane event or a higher
52 exposure (Zhang et al. ~~in revision~~2022b).

53 The recovery from hurricanes also depends on many factors, such as the disturbance severity (Walker 1991;
54 Everham and Brokaw 1996; Cole et al. 2014; Heartsill Scalley 2017) and traits of individual species (Curran et al.
55 2008; Lewis and Bannar-Martin 2011). Species with lower wood density have ~~a faster resprouting~~shorter times to
56 resprout (Paz et al. 2018), higher growth rate (King et al. 2006), and shorter biomass recovery times (Curran et al.
57 2008). The number of resprouts~~ing~~ of some species further varies with time since disturbance (Brokaw 1998; ~~Zhang~~
58 ~~et al. in revision~~). Less severe disturbances lead to a faster recovery and a higher recovery equilibrium of stem density
59 and aboveground biomass compared to the level observed prior to the disturbance (Wang and Eltahir 2000; Parker et
60 al. 2018). For example, observations on a tropical forest canopy in western Mexico after two hurricanes—category 2
61 Jova and category 4 Patricia—showed that hurricane Jova destroyed 11% of the aboveground biomass while hurricane
62 Patricia destroyed 23%; the recovery was more rapid after the less intense hurricane Jova (Parker et al. 2018). ~~Wang~~
63 ~~and Eltahir (2000) provided theoretical and numerical analyses on multiple equilibrium nature of a regional climate~~
64 ~~system. Their results showed that the recovery speed and the equilibrium state of the coupled biosphere-atmosphere~~
65 ~~system are sensitive to the initial vegetation condition impacted by disturbances.~~

66 Although the immediate mortality and subsequent recovery of tropical forest from hurricane disturbances
67 have been thoroughly studied via observations, the long-term effects of consecutive hurricane disturbances on tropical
68 forests have rarely been studied. Models that can simulate the immediate mortality and subsequent recovery of an
69 ecosystem can play a role in understanding potential mechanisms driving the mortality and recovery of the ecosystems
70 and studying the long-term effects of disturbances, particularly if the nature of the disturbances is changing with
71 climate. Uriarte et al. (2009) implemented hurricane disturbance in a forest simulator and investigated the long-term
72 dynamics of forest composition, diversity, and structure. However, the biological and environmental processes of the
73 forest simulator used are not dynamic and thus the model cannot simulate the adaptation of vegetation to the changes
74 of environment (Jorgensen 2008). Vegetation dynamics models can account for changes in the ecosystem resulting
75 from a changing environment (Medvigy et al. 2009; Longo et al. 2019b), and further allow us to explore scenarios via
76 synthetic experiments and thus emulate what might happen in forests under novel environmental conditions. For
77 example, Feng et al. (2018) used the Ecosystem Demography model (ED2) (Moorcroft et al. 2001) to study the impact
78 of climate change on the forest studied in Uriarte et al. (2009). The ED2 model is a process-based vegetation dynamics
79 model, it represents the size and age structure of the forest, and thus the model can represent the observed differential
80 impact from disturbances (such as fire, drought, insects, land use change, and natural disturbances) across plants of
81 different functional groups and size classes (Medvigy et al. 2012; Zhang et al. 2015; Miller et al. 2016, Trugman et

82 al. 2016). However, the impacts of hurricane disturbances have not been implemented in vegetation dynamics models,
83 and thus the long-term effects on the forest of a changing hurricane regime have not been investigated.

84 As mortality and recovery vary with species, the species composition of the forest is affected by hurricane
85 disturbances. In modeling studies, it is impractical to incorporate each and individual species (tens and hundreds). To
86 address variation in species diversity, ~~In the past decades,~~ there has been a strong effort ~~in the past decades~~ to
87 incorporate functional diversity in ~~terrestrial biosphere~~ vegetation dynamics models (Moorcroft et al. 2001;
88 Sakschewski et al. 2016; Fisher et al. 2018; Fisher and Koven 2020). This effort acknowledges the variability in traits
89 and trade-offs of species that exist in tropical forests (e.g., Baraloto et al. 2010). Three plant functional types (PFT)
90 are identified for the species in tropical forests during a secondary succession after a disturbance; they are early, mid,
91 and late successional PFTs (hereafter Early, Mid, and Late PFTs), corresponding to the three successional stages
92 during the secondary succession (Kammesheidt 2000). Specifically, Early PFT dominates the early successional stage
93 of the recovery, it includes ~~F~~fast growing pioneer species that have low wood density, establish and recruit in open
94 gaps formed after disturbances and grow rapidly in the high light environment. ~~They dominate the early successional~~
95 stage of the recovery, and thus are categorized as ~~Early plant functional type (PFT).~~ Mid PFT dominates the mid
96 successional stage after a disturbance, and includes ~~S~~species that have intermediate growth and are somewhat shade
97 tolerant, ~~dominate the plant community in the mid successional stage after a disturbance, and thus are categorized as~~
98 ~~Mid PFT.~~ Late PFT dominates the late successional stage and includes speciesSpecies that have slow growth and are
99 shade tolerant ~~dominate a plant community in the late successional stage after a disturbance, and thus are categorized~~
100 as ~~Late PFT.~~ Using three PFTs is also a compromise between representing a range of life strategies while not adding
101 too much complexity in model parameterizations (Moorcroft et al. 2001; Medlyn et al. 2005).

102 One important and distinct species in tropical forests in the Caribbean islands is the palm species *Prestoea*
103 *montana* (Sierra palm). Many studies in the Luquillo Mountains have either excluded palms from analysis
104 (Zimmerman et al. 1994) or treated palms separately from other trees (Zimmerman et al. 1994; Uriarte et al. 2009), as
105 indeed they are monocots, not dicots like the other trees in the forest. A previous study that simulates the response of
106 the forests in the Luquillo Mountains to climate change using the ED2 model categorized the palm species as a Late
107 PFT tree (Feng et al. 2018). However, there are important differences. ~~The palms species is~~ are more resistant to
108 hurricane damage as compared to trees (Francis and Gillespie 1993; Uriarte et al. 2019) and are more resilient to
109 hurricane disturbances due to their -. Moreover, the palm species cannot be classified into one of the successional PFTs,
110 because palms possess some early successional traits, such as low "wood" density and high fecundity under open
111 canopy (Lugo and Rivera Batlle 1987; Lugo et al. 1998), ~~that allow them to recruit quickly when the canopy opens~~
112 (Zhang et al. in revision); and some late successional traits, such as and have high tolerance to shade (Ma et al. 2015);
113 that allow them to thrive when the canopy closes (Zhang et al. in revision). ~~To account for these unique~~
114 characteristics All those characteristics separate palms from other trees and favor the survival of palms after hurricane
115 disturbances. We believe palms cannot be categorized into one of the existent PFT categories in the model, and hence
116 we define a new ~~Palm~~ PFT —Palm.

117 In this paper, we describe the implementation of hurricane mortality and recovery modules that account for
118 the variation with disturbance severity, forest resistance state, PFT and diameter size of individual stems in the

119 Ecosystem Demography model (ED2). The model is then used to study the recovery of a tropical rainforest after
120 hurricane disturbances. The results indicate that a scenario with a single hurricane disturbance has little long-term
121 impact on forest structure and composition but enhances the aboveground biomass accumulation of a tropical
122 rainforest, relative to a no hurricane disturbance scenario.

123 **2 Methods and Materials**

124 **2.1 Census Observations**

125 Tree censuses were carried out at Bisley Experimental Watersheds (BEW) in the Luquillo Experimental Forest in
126 Puerto Rico starting in 1989, three months before hurricane Hugo (pre-Hugo 1989), and repeated three months after
127 hurricane Hugo (post-Hugo 1989), and then every five years since then (1994, 1999, 2004, 2009, 2014). The census
128 recorded the diameter at breast height (1.3m) (DBH) and species of each stem with DBH \geq 2.5 cm and height (H) of
129 selected stems in 85 permanent forest dynamics plots in the forest. Each plot is a 10-meter diameter circle and plots
130 are 40 meters apart extending 13 hectares. The last census was conducted three months after hurricane Maria and
131 recorded auxiliary damage information of each stem. The detailed description of the study site and the census
132 observations can be found in Zhang et al. (2022b) and the census data between 1989 and 2014 are from Zhang et al.
133 (2022a) and the post-Maria census data are from Zhang et al. (2020). Following Zhang et al. (2022b), species are
134 categorized into four PFTs according to their successional status based on previous studies (Walker 1991; Schowalter
135 and Ganio 1999; Uriarte et al. 2005; Muscarella et al. 2013; Heartsill Scalley 2017; Feng et al. 2018): early, mid, late
136 successional tropical trees, and palms (Early, Mid, Late, and Palm PFT, respectively). The stem density, DBH growth
137 rate, and basal area are calculated from the census data for each PFT in each census. The aboveground biomass (AGB)
138 of Early, Mid, and Late PFTs are estimated from DBH using the AGB-DBH relationship from Scatena et al. (1993);
139 the AGB of Palm PFT is estimated from the AGB-Height relationship of *P. montana* from Scatena et al. (1993) and
140 the Height-DBH relationship of Palm PFT from the census observations at our study site (Section 2.2.2).

141 **2.1.2 Model Description**

142 The Ecosystem Demography model (ED) is a cohort-based model, and it describes the growth, reproduction, and
143 mortality of each cohort in each patch in a forest site. A cohort is a group of stems with the same PFT and similar
144 diameter size and age. A patch is an area with the same environmental condition and disturbance history. A cohort
145 accumulates carbon through photosynthesis, and the net accumulated carbon (i.e., gross primary productivity minus
146 respiration and maintenance of living tissues) will be used for growth and reproduction. When a cohort is mature,
147 reaching the maturity reproductive height (e.g., 18 m), the cohort will allocate a portion of carbon to reproduction
148 (e.g., 30% of net carbon accumulation to seeds, flowers, and fruits), and the rest of the net accumulated carbon will
149 be used for structural growth. Structural growth is quantified by the increase of DBH through structural biomass-DBH
150 allometries; stem height, leaf biomass, and crown area are then scaled given the H-DBH, leaf biomass-DBH, and
151 crown-DBH allometries. Each cohort will also experience mortality from multiple factors, including aging,
152 competition, and disturbance, which will be described in detail in Section 2.3.2.

153 The model simulates transient fluxes of carbon, water, and energy during short-term physiological responses
154 and long-term ecosystem composition and structure responses to changes in environmental conditions. The second
155 version of the ED model, ED2, modifies the calculations of radiation and evapotranspiration of the original ED model,
156 leading to a more realistic long-term response of ecosystem composition and structure to atmospheric forcing
157 (Medvigy et al. 2009; Longo et al. 2019b). Details of the ED and ED2 models can be found in Moorcroft et al. (2001),
158 Medvigy et al. (2009), and Longo et al. (2019a). Here we add a new PFT (Palm) and implement hurricane disturbance
159 in the ED2 model, and we name it ED2-HuDi V1.0.

160 2.1.12.2.1 Adding Palm as a New PFT

161 The standard ED2 model represents a variety of broadleaf trees, needleleaf trees, grasses and lianas (Albani et al.
162 2006; Medvidy et al. 2009; Longo et al. 2019a; di Porcia e Brugnera et al. 2019). Yet, to date, none of the existing
163 PFTs describe the traits of palms, even though palms are a globally abundant component of tropical forests (Muscarella
164 et al. 2020). ~~Since there is little knowledge about the traits of Palm.~~ We do know that ~~palms have low “wood density”~~
165 ~~of -0.25 g cm^{-3} (Zanne et al. 2009; Chave et al. 2009) and the palm species that occurs at our study site (*Prestoea*~~
166 ~~*montana*) has a low wood density of 0.31 g cm^{-3} (Swenson and Umana 2015) and it grows fast in open canopies like~~
167 early successional tropical trees (Lugo and Rivera Batlle 1987; Lugo et al. 1998) and are tolerant to shade like late
168 successional tropical trees (Ma et al. 2015; Zhang et al. in revision). Hence, we assume that the physiological traits of
169 Palm have the same probability distributions as those of ~~late tropical trees~~ Late PFT except for wood density which is
170 assumed the same as that of ~~early tropical trees~~ Early PFT. The allometries of Palm are discussed separately in the next
171 section.

172 2.1.12.2.2 Modifying the Allometric Relationship

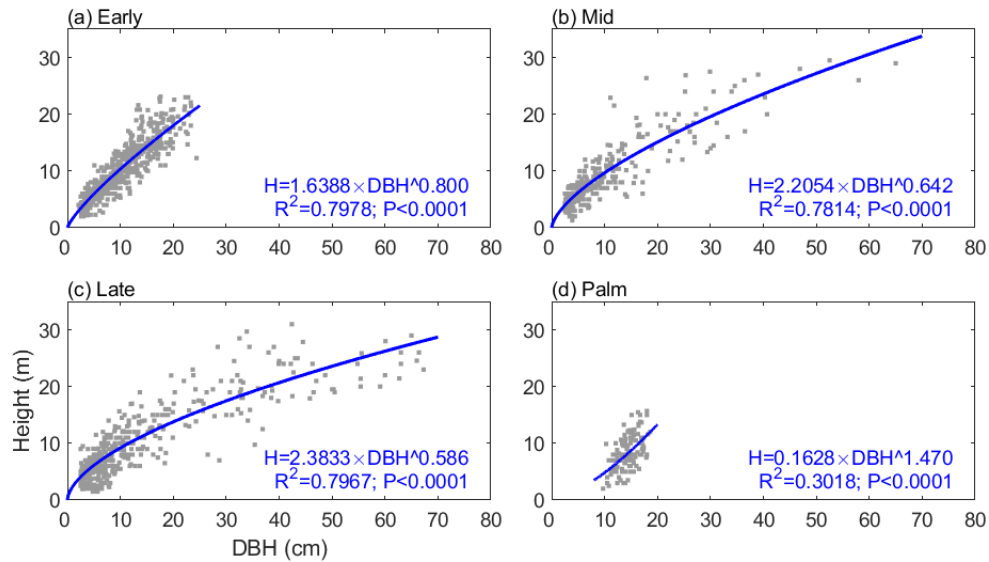
173 The H-DBH allometric relationships between stem height (H; m) and diameter at breast height (DBH; cm) for four
174 tropical PFTs (Early, Mid, Late, and Palm) come from census data at ~~Bisley Experimental Watersheds (BEW)~~ in the
175 Luquillo Experimental Forest in Puerto Rico (Zhang et al. 2022a). The relationships take the form,

$$176 \quad H = a DBH^b, \quad (1)$$

177 where a and b are PFT-specific scale and shape parameters (Zhang et al. in revision; Figure 1). The diameter range for
178 the Palm PFT is between 10 and 20 cm while that for the tree PFTs is between 2.5 and 90 cm. The scale parameter a
179 is 1.6388, 2.2054, 2.3833, and 0.1628 for Early, Mid, Late, and Palm PFT, respectively. The shape parameter b ~~for~~
180 ~~the four PFTs are~~ is 0.80, 0.64, 0.59, and 1.47 for the four PFTs (Table S1). Palm has a smaller scale parameter and a
181 significantly larger shape parameter, demonstrating that palms are shorter than other PFTs given the same DBH. The
182 constrained diameter range and the H-DBH allometry of Palm makes it difficult for palms to access sunlight and
183 would normally prevent them from establishing in the ED2 model. A previous study implementing liana to the ED2
184 model also experienced similar issues (di Porcia e Brugnera et al. 2019). They ~~then were to use~~ used an allometry for
185 liana with DBH between 3 and 20 cm and then for lianas with DBH less than 3 cm, they used the allometry of early
186 successional trees ~~for lianas with DBH less than 3 cm~~ (di Porcia e Brugnera et al. 2019). Following a similar approach
and to make sure Palm has reasonable opportunity to compete with a reasonable diameter range, we assume that the

187 minimum height of Palm in the model is 4.8 m (corresponding to 10 cm DBH of Palm; other PFTs have a minimum
 188 height of 1.5 m for recruitment), and when Palm grows to a height of 18 m (corresponding to 20 cm DBH)—maximum
 189 height observed for the Palm in the forest (Figure 1)—, they will allocate all the carbon to reproduction instead of
 190 growth (relative allocation to reproduction is 1 for Palm, and 0.3 for other PFTs) (Table S1).

191 For other allometric relationships, such as leaf biomass-DBH, structural biomass-DBH, and crown area-DBH
 192 relationships, we used the model default for Early, Mid, and Late PFTs, and assumed that Palm has the same
 193 relationships as Early (Figure S1).



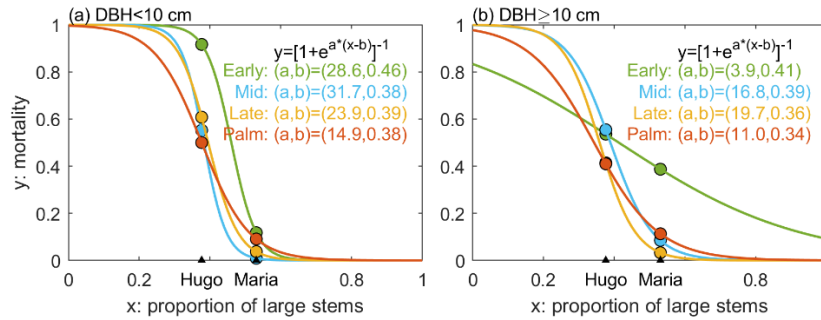
194
 195 **Figure 1.** The height-diameter (DBH) relationship for the four PFTs: (a) Early, (b) Mid, (c) Late, and (d) Palm. The gray dots are
 196 observations with outliers removed (Supplementary Information S1) and the blue lines are the estimated height-DBH relationship
 197 based on these observations. The height-DBH model and the corresponding coefficient of determination (R^2) and p-value for each
 198 PFT are given at the bottom of each panel.

199

200 **2.1.32.2.3 Implementing Hurricane Disturbance**

201 The ED2 model accounts for several types of disturbances, such as fires, land use, logging (Albani et al. 2006; Longo
 202 et al. 2019a), but not hurricane disturbance. To account for hurricane impacts, we implement a hurricane-induced
 203 wind mortality module and a seedling recovery module in the model. The wind mortality module consists of two
 204 parts—the disturbance rate of the forest area (λ_d) and the survivorship of each cohort (s_c) in the disturbed areas. For
 205 any patch with pre-disturbance area A , the area that is affected by disturbance (A_d) is proportional to λ_d , following
 206 Moorcroft et al. (2001): $A_d = A [1 - \exp(-\lambda_d \Delta t)]$. The disturbed area (A_d) will be disturbed and become a new patch
 207 (age 0), and the population within the new patch will be determined by the survivorship to disturbance. The remaining
 208 area ($A - A_d$) will remain undisturbed, and the stem density will remain unchanged. The disturbance rate (λ_d) is the ratio
 209 of the area disturbed to the total area of the forest and it is a constant across patches.—The survivorship of each cohort
 210 (s_c) is the ratio of the cohort density that survived after the disturbance to the cohort density before the disturbance,
 211 and it is cohort dependent. The cohorts that survived in disturbed areas will make up a the new patch with area equal
 212 to the disturbed area (age 0). In this study, we assume that the forest is fully disturbed and $\lambda_d = 1$. The survivorship

213 of each cohort s_c is calculated as $s_c = 1 - \lambda_c$, where λ_c is the mortality of each cohort. Based on previous analyses, λ_c
 214 varies with hurricane strength, forest structure, the PFT category and the DBH size of the cohort (Zhang et al. [in](#)
 215 [revision2022b](#)). First, we implement a binary model for the mortality with respect to hurricane wind, where mortality
 216 occurs when hurricane wind exceeds a threshold and no mortality otherwise. This binary model is built on the binary
 217 relationship between hurricane-induced forest damage and hurricane wind speed from nine hurricane events at BEW
 218 between 1989 and 2017 (Supplementary Information [S1S2](#), [S2S3](#), and [S3S4](#)). The wind speed threshold was set at 41
 219 $m s^{-1}$ because the strongest hurricane wind that caused no damage to the forest at BEW was 40 $m s^{-1}$ from hurricane
 220 Georges in 1998 and the lowest wind speed that caused damage to the forest was 42 $m s^{-1}$ from hurricane Maria in
 221 2017 (Supplementary Information [S1S2](#), [S2S3](#), and [S3S4](#)). Given-If mortality occurs (i.e., wind speed exceeds the
 222 threshold), the mortality rate of each cohort (λ_c) is a continuous function of the size structure of the forest, represented
 223 by the proportion of large stems (DBH ≥ 10 cm) to the total recruited stems (DBH ≥ 2.5 cm). Figure [1-2](#) shows the
 224 mortality of each PFT and DBH class during two hurricane events (Hugo and Maria) based on census observations at
 225 BEW (see Section [2.1-2-2](#)). We fit a logistic function to the mortality-structure pair of each PFT and DBH class based
 226 on the observed pairs of mortality and structure from the two hurricane events.



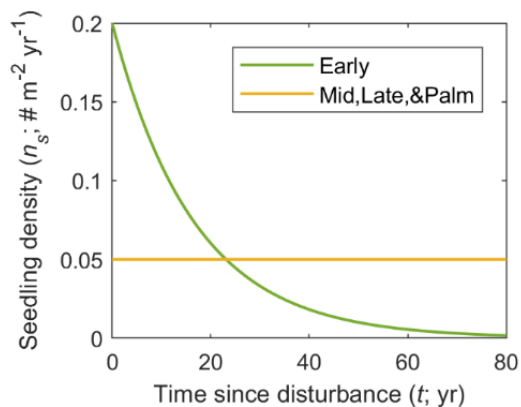
227
 228 **Figure 21.** The mortality for each PFT and DBH class. The mortality as a function of the size structure of the forest for each PFT
 229 and DBH class. The size structure is represented as the proportion of large stems (DBH ≥ 10 cm) to the total number of stems in
 230 the forest (DBH ≥ 2.5 cm). The dots represent observed mortality and proportion of large stems pairs from hurricane Hugo and
 231 hurricane Maria (Zhang et al. [in revision2022b](#)). Four colors represent four PFTs. The solid lines represent the estimated mortality
 232 as a logistic function of the proportion of large stems. The panel on the left is for small stems and that on the right is for large stems.

233
 234 Hurricanes not only cause immediate stem mortality, but also affect the establishment of seedlings by opening
 235 the canopy ([Everham 1996](#); [Brokaw 1998](#); [Uriarte et al. 2009](#); [Uriarte et al. 2012](#)). Brokaw (1998) pointed out that
 236 hurricanes promote germination and seedling establishment of the early successional species *C. schreberiana*, and
 237 that the seedling establishment ends shortly after the disturbance as the canopy closes. The census data at BEW also
 238 show abundant recruitments of the Early PFT in the first 20 years after hurricane Hugo and decreasing recruitment
 239 with time (Zhang et al. [in revision2022a](#)). Therefore, based on the recruitment of Early PFT from the census data
 240 (Zhang et al. 2022a), we implement a recovery module where the seedling density from seed rain (n_s ; individuals m^{-2}
 241 yr^{-1}) decreases with time since the last disturbance, and the reduction varies with PFT categories as:

$$n_s = n_0 \exp(-\alpha t), \quad (2)$$

242 where n_s is the seedling density t years after last hurricane disturbance, n_0 and α are PFT-dependent parameters.
 243 Specifically, Mid, Late, and Palm PFTs maintain a low but constant seedling density ($n_0 = 0.05$ individuals $m^{-2} yr^{-1}$)

244 and $\alpha = 0 \text{ yr}^{-1}$). The Early PFT has high seedling density ($n_0 = 0.2 \text{ individuals m}^{-2} \text{ yr}^{-1}$) shortly after a hurricane
 245 disturbance and the seedling rate decreases to the same value as other PFTs about 20 years after the disturbance ($\alpha =$
 246 0.06 yr^{-1}), and it continues to decrease thereafter (Figure 23).



247
 248 **Figure 23.** The seedling density for each PFT after a disturbance.

249
 250 **2.2 — Census Observations**

251 ~~Tree censuses were carried out in BEW in the Luquillo Experimental Forest in Puerto Rico starting in 1989, three~~
 252 ~~months before hurricane Hugo (pre Hugo 1989), and repeated three months after hurricane Hugo (post Hugo 1989),~~
 253 ~~and then every five years since then (1994, 1999, 2004, 2009, 2014). The census recorded the diameter at breast height~~
 254 ~~(DBH) and species of each stem with $\text{DBH} \geq 2.5 \text{ cm}$ in 85 dynamics plots in the forest. The last census was conducted~~
 255 ~~three months after hurricane Maria, and recorded auxiliary damage information of each stem. The detailed description~~
 256 ~~of the study site and the census observations can be found in Zhang et al. (in review) and the census data between~~
 257 ~~1989 and 2014 are from Zhang et al. (in review) and the post Maria census data are from (Zhang et al. 2020). Species~~
 258 ~~are categorized into four PFTs: early, mid, late successional tropical trees, and palms (Early, Mid, Late, and Palm~~
 259 ~~PFT, respectively) following Zhang et al. (in review). The stem density, DBH growth rate, and basal area are calculated~~
 260 ~~from the census data for each PFT in each census, and the aboveground biomass is estimated from DBH using the~~
 261 ~~allometric relationship from Scatena et al. (1993). The census observations will be used for initializing, calibrating,~~
 262 ~~and validating model simulations.~~

263 **2.3 Model Calibration and Validation**

264 **2.3.1 The GLUE approach**

265 The concept of Generalized Likelihood Uncertainty Estimates (GLUE) (Binley and Beven 1991; Beven and Binley
 266 1992; Mirzaei et al. 2015) has been widely used to calibrate parameters in complex hydrological models. The steps of
 267 GLUE include 1) generating a number of samples of the parameter set from a prior distribution of the parameters, 2)
 268 running the simulation for each parameter set, 3) choosing a likelihood function (or weight function) to calculate the
 269 weight of each simulation based on observations and the estimated outputs from the model simulation, and 4) selecting

270 the optimal parameter set and estimating the posterior distribution of the parameters and the posterior distribution of
271 the output variables. Here we use GLUE, for the first time, to calibrate the parameters in the ED2 model.

272 To obtain the prior distribution of parameters, we build on a previous parameter sensitivity analysis using the
273 ED2 model for a nearby forest in Puerto Rico by Feng et al. (2018). They demonstrated that model simulations are
274 sensitive to ten parameters, listed in Table 1, and provided the posterior mean and 95% confidence limits of the
275 parameters calibrated from plant traits observations using the Predictive Ecosystem Analyzer (PEcAn; LeBauer et al.
276 2013). We select the same parameters and use the posterior distribution of those parameters from Feng et al. (2018)
277 as the prior distribution for the GLUE in our study. We cannot just use their parameter distributions as final results
278 because our implementation has a site-specific set of allometric equations, explicitly represents palms as a separate
279 PFT and considers hurricane disturbances ([Sect. 2.1](#)[Section 2.2](#)). Feng et al. (2018) reported only the mean and the
280 upper and lower 95% confidence limits of the parameters (not the entire distribution), we assume that the parameters
281 have lognormal distributions. For the Palm PFT, we assume that it has the same distributions as Late, except that the
282 woody tissue density of Palm has the same distribution as that of Early. ~~The dark respiration factor from Feng et al.~~
283 ~~(2018) has a too wide range (Wang et al. 2013), and thus~~ From a different study system, Wang et al. (2013) constrained
284 the dark respiration factor from 0.01–0.03 to 0.01–0.016 by assimilating observations of model output variables.
285 Following Wang et al. (2013), we restrict the dark respiration factor to a smaller range with a uniform distribution
286 between 0.005 and 0.0175 for each PFT. Consistent with Meunier et al. ([in revision 2022](#)), we found that model results
287 are also sensitive to the parameter clumping factor (Figure S2). Therefore, we add the parameter of clumping to the
288 set being calibrated. Clumping factor is ~~the ratio of effective LAI to the total LAI~~ defined as the projected area of
289 leaves per unit ground area and affects the transmission of radiation (Chen and Black 1992); it ranges from zero to
290 one with zero representing leaves clumped in a single point (0-area) and one representing leaves uniformly distributed
291 in the unit area. Because of tree crowns, branches, and subbranches, leaves of plant canopy are not uniformly
292 distributed per unit area nor clumped at a single point. We assume that the clumping factor is the same for all PFTs
293 and the distribution of the clumping factor is uniform between 0.2 and 0.8.

294 We sample 10,000 realizations for the 41 parameters (10 parameters for each of the four PFTs and the one
295 clumping parameter for all PFTs) using the Latin Hypercube Sampling method embedded in MATLAB (Stein 1987).
296 We initialize the model with the pre-Hugo 1989 observations and run the model for 29 years, corresponding to 1989–
297 2018. The first 25 years (1989–2014) are used to calibrate the model with observations and the last four years (2015–
298 2018) for validation. We tested different calibration lengths (1989–1999, 1989–2004, and 1989–2009). 1989–2009
299 calibration period gives the same optimal simulation as 1989–2014 calibration period (Figure 4), but shorter
300 calibration lengths 1989–1999 (Figure S3) and 1989–2004 (Figure S4) throw away critical recovery information and
301 cannot give robust simulation in the validation period. We calculate the mean squared errors (*MSE*) of each realization
302 ($j, j=1, 2, \dots, 10,000$) for the calibration period,

$$MSE_j = \frac{1}{nm} \sum_{t=1}^m \sum_{i=1}^n \left(\frac{X_{i,t,j} - Y_{i,t}}{\frac{1}{m} \sum_{t=1}^m Y_{i,t}} \right)^2, \quad (3)$$

303 where $X_{i,t,j}$ represents the j^{th} model simulations for variable i at time t , and $Y_{i,t}$ represents observations for variable i at
304 time t . The variables used to calculate *MSE* are stem density (individuals m^{-2}), average DBH growth rate (cm (5

305 yr^{-1}), and basal area (BA) ($\text{cm}^2 \text{m}^{-2}$) for the four PFTs ($n=12$) (Figure 34). Times are the six census years ($m=6$)
 306 with observations before hurricane Maria: post-Hugo 1989, 1994, 1999, 2004, 2009, 2014. Because BA is directly
 307 calculated from the DBH of each cohort and weighted by the stem density of the cohort, the size structure (distribution
 308 of stem DBHs) of the forest is implicitly represented with the variables overall stem density and total BA. Moreover,
 309 the PFT composition is explicitly represented with the PFT-specific variables. Therefore, the *MSE* metric implicitly
 310 measures the performance of a realization in describing the observed time series of the forest's size structure and PFT
 311 composition.

312 We select the simulation with the smallest *MSE* as the optimal simulation and the corresponding parameter
 313 set as the optimal parameter set. To obtain the posterior distribution of parameters, we first calculate the weight
 314 (likelihood) of each realization following Binley and Beven (1991),

$$w_j = \text{MSE}_j^{-K}, \quad (4)$$

315 which is then rescaled to sum to one ($w_j / \sum_{j=1}^N w_j$), where K is the parameter that controls the weight of each
 316 realization. When $K = 0$, every simulation will have equal weights and when $K = \infty$, the single best simulation will
 317 have a rescaled weight of 1 while all others being zero. We select K such that the weighted standard deviations from
 318 simulations are within and overlap as much as possible with the standard deviations of observations, indicating that
 319 the parameters in those weighted simulations are reasonable given the uncertainty of the observations (Freer et al.
 320 1996). The weighted standard deviation of variable X is calculated as

$$\sigma_X = \sqrt{\sum_{j=1}^N w_j (X_j - m_X)^2}, \quad (5)$$

321 where $m_X = \sum_{j=1}^N w_j X_j$ is the weighted mean of the simulated variable. We find that $K=8$ has the best performance
 322 on the posterior estimates of output variables stem density, aboveground biomass, basal area, proportion of each PFT,
 323 and proportion of large stems (Figure 34, Figure S3S5, and Figure S4S6). Lastly, the posterior empirical cumulative
 324 distribution function (CDF) of the parameters is obtained as

$$F(P \leq p) = \sum_{j:P_j \leq p} w_j. \quad (6)$$

325 The posterior empirical CDFs are then fit to lognormal distributions.

326 2.3.2 Non-Hurricane Mortality

327 The non-hurricane mortality of ~~pal~~alm-Palm is not well represented in the model (Figure S5S7), as initially calibrated.
 328 The observed non-hurricane mortality is an overall mortality regardless of the cause of the death and is calculated
 329 from non-hurricane censuses, whereas the non-hurricane mortality in model simulations includes aging mortality,
 330 competition mortality, and disturbance mortality. We turned off all disturbances except for hurricane disturbance and
 331 treefall disturbance. The disturbance mortality includes the background exogenous mortality ~~rate (0.014 year⁻¹ for~~
 332 ~~small stems)~~, and treefall disturbance rate ~~(0.0126 year⁻¹ for small stems and 0.014 year⁻¹ for large stems)~~. Background
 333 mortality rate is 0.014 yr⁻¹ for small trees and zero for large trees because, following Moorcroft et al. (2001), this
 334 mortality is accounted for in the treefall disturbance rate (i.e., the background mortality of large trees is what causes
 335 the treefall disturbance). The treefall disturbance rate mortality is a combination of the area impacted by treefall

336 disturbance and the survivorship of this disturbance. By default, in ED2, it is assumed that the treefall disturbance rate
337 is 0.014 yr⁻¹, survivorship to treefall disturbance is zero for large trees and 10% for small trees, and thus overall treefall
338 mortality is 0.014 yr⁻¹ for large trees and 0.0126 yr⁻¹ for small trees. Competition mortality is related to carbon
339 starvation (i.e., negative net carbon accumulation) ~~the negative carbon balance~~ due to light and water limitation and
340 varies with cohorts. Aging mortality is the reciprocal of the longevity of the cohort without any biotic and abiotic
341 influences, and it is modeled as a constant for each PFT depending on the wood density of the PFT (ρ_{PFT}) relative to
342 the wood density of the Late PFT (ρ_{Late}): $0.15 \times (1 - \rho_{PFT}/\rho_{LATE})$ (Moorcroft et al. 2001). Since Palm has a much lower
343 “wood” density (~~-0.25-0.31~~ g cm⁻³; Swenson and Umana 2015) than the Late PFT (model default 0.9 g cm⁻³), the
344 aging mortality of Palm is ~~~0.1 year⁻¹yr⁻¹~~, or the longevity of palms would be equivalent to ~10 years. However, this
345 is in contrast to the average age of the palm species in the Luquillo Experimental Forest, which was found to be 61.1
346 years and the oldest palms were more than 100 years old in 1982 (Lugo and Rivera Batlle 1987). This suggests that
347 the aging mortality of Palm calculated from its woody tissue density is a drastic overestimation. Therefore, we assume
348 that the aging mortality of Palm is independent of its woody tissue density and is 0 ~~year⁻¹yr⁻¹~~, same as that of Late.

349 With a lower mortality (decreasing aging mortality from ~0.1 to 0), the density of Palm increases
350 continuously in the forest because of continuously recruiting seedlings, while the density of other PFTs and the AGB
351 of all PFTs are less affected (Figure S6S8). A previous study showed that hurricane disturbance can result in an
352 increase in seed production in the palm species (Gregory and Sabat 1996). Therefore, we calibrate the seedling
353 recovery module of Palm that we implemented in Section 2.2.3-2.1.3. Specifically, we test several recovery seedling
354 densities (Eq. (2)) for Palm, assuming that the seedling density of Palm is similar to that of Early—decreasing with
355 time since disturbance—but with different starting seedling level (n_0) and decaying factor (α). We tested 36
356 combinations of n_0 varying from 0 to 0.05 individuals m⁻² yr⁻¹ with interval 0.01 individuals m⁻² yr⁻¹ and α varying
357 from 0 to 0.05 yr⁻¹ with interval 0.01 yr⁻¹. We found that five of them lead to a smaller *MSE* (Eq. (3)) than the GLUE
358 optimal simulation (0.1678, 0.1662, 0.1642, 0.1646, and 0.1691 for the five experiments and 0.1803 for the GLUE
359 optimal), and the five combinations have the same starting seedling density ($n_0=0.02$ individuals m⁻² yr⁻¹) but different
360 values of the decaying factor ($\alpha=0.01, 0.02, 0.03, 0.04, \text{ and } 0.05$ yr⁻¹, respectively) (Figure S7S9). To choose from the
361 five decaying values, we compared the recovery density schemes with the observed recruitment of Palms—(stems
362 entering the census with DBH ≥ 2.5 cm and H ≥ 1.5 m each year). As we do not have seedlings but only recruited
363 stems in our census data, we assumed that seedling density has the same response (varying with time since disturbance)
364 as recruitment, but not necessarily the same magnitude (density) as recruitment. Based on the census data, ~~T~~here were
365 37, 64, 50, 34, and 32 palms recruited in the 85 plots (78.5 m² each plot) in 1994, 1999, 2004, 2009, and 2014 censuses,
366 respectively, which corresponds to 0.0011, 0.0019, 0.0015, 0.0010, and 0.0010 individuals m⁻² yr⁻¹ after 5, 10, 15, 20,
367 and 25 years of the Hugo disturbance. In other words, the recruitment decreases to half of the starting level in 20–25
368 years, or a decaying factor $\alpha \approx 0.03$ yr⁻¹. We assume that the seedling density has the same decaying rate as the
369 recruitment density and thus we select the seedling density scheme $n_0=0.02$ individuals m⁻² yr⁻¹ and $\alpha=0.03$ yr⁻¹ as the
370 seedling recovery scheme for Palm.

371 After changing the aging mortality of Palm to zero and the seedling density to a lower and slowly decreasing
372 value, we did not repeat the GLUE. This is because Palm has constrained DBH size (between 10 and 25 cm) and

373 decreasing the aging mortality increases its density while decreasing seedling reproduction decreases its density,
 374 which maintains the overall density of Palm, without affecting other variables of Palm nor variables of other PFTs
 375 (Figure S7S9). Therefore, we use the parameter set found from the GLUE (Table 1) but with 0-aging mortality and a
 376 lower seedling density recovery ($n_0=0.02$ individuals $m^{-2} yr^{-1}$ and $\alpha=0.03 yr^{-1}$) for simulations in the following studies.

377 2.4 Parameter Sensitivity Analyses and Variance Decomposition

378 Using a similar approach to PEcAn (LeBauer et al. 2013), we analyze the sensitivity of model simulations to the
 379 parameters and the contribution of the parameters to the variances. Specifically, we set up nine experiments for each
 380 of the 41 parameters, corresponding to the nine quantiles (10th, 20th, ..., 90th) of the posterior distribution of each
 381 parameter, while all other parameters remain constant at their optimal. For the total 369 sensitivity experiments, we
 382 initialize the model with the pre-Hugo observation and run each experiment for 25 years (1989–2014).

383 To study the stability of the optimal parameter set, we calculate the *MSE* of each experiment and compare it
 384 with the *MSE* of the optimal. To quantitatively study the sensitivity of output variables to the parameters, we calculate
 385 the standardized cubic regression coefficient (β),

$$\beta = \frac{\partial \tilde{x}(p_o)}{\partial p_o} \bigg/ \frac{x_o}{p_o}, \quad (7)$$

386 where p and x are a specific parameter and the corresponding output variable. \tilde{x} is the cubic regression function of x
 387 on p : $\tilde{x} = ap^3 + bp^2 + cp + d$, estimated from the pairs of parameter p and variable x along the nine quantiles of the
 388 posterior distribution of parameter p . $\frac{\partial \tilde{x}(p_o)}{\partial p_o}$ is the partial derivative of \tilde{x} on p at p_o , where p_o and x_o are the optimal
 389 value of the parameter and the corresponding output variable. Only when the R^2 metrics of the regression function is
 390 significant at 99% confidence level via student- t test is β calculated. We calculate β for 20 variables [stem density,
 391 BA, AGB, and leaf area index (LAI) of each PFT and of all PFTs] and for the 41 parameters. The β for the variables
 392 at the first and the 25th simulation years are selected to represent the short-term and long-term response of modeled
 393 variables to the parameters, respectively.

394 To quantitatively study the uncertainty of the simulated variables (stem density, AGB, BA, LAI, etc.) from
 395 the uncertainties of the parameters, we calculate the coefficient of variation (θ) for each variable resulting from
 396 experiments with different parameters:

$$\theta = \frac{\sigma}{\mu}, \quad (8)$$

397 where σ and μ are the standard deviation and the mean value of the variable from the nine experiments of the parameter.
 398 To study the contribution of each parameter to the uncertainties of the simulated variables, we calculate the total
 399 variance from all the sensitivity experiments (Var_T) and the variance from experiments of each parameter (Var_p), and
 400 decompose the total variance as follows,

$$Var_T = \sum_{p=1}^{Np} Var_p + \omega, \quad (9)$$

401 where Var_p is the variance of the model outputs from experiments with different values of parameter p , and Np is the
 402 total number of parameters ($Np=41$), ω represents the variance from the interaction among parameters.

403 2.5 Experiments with Different Initial Conditions

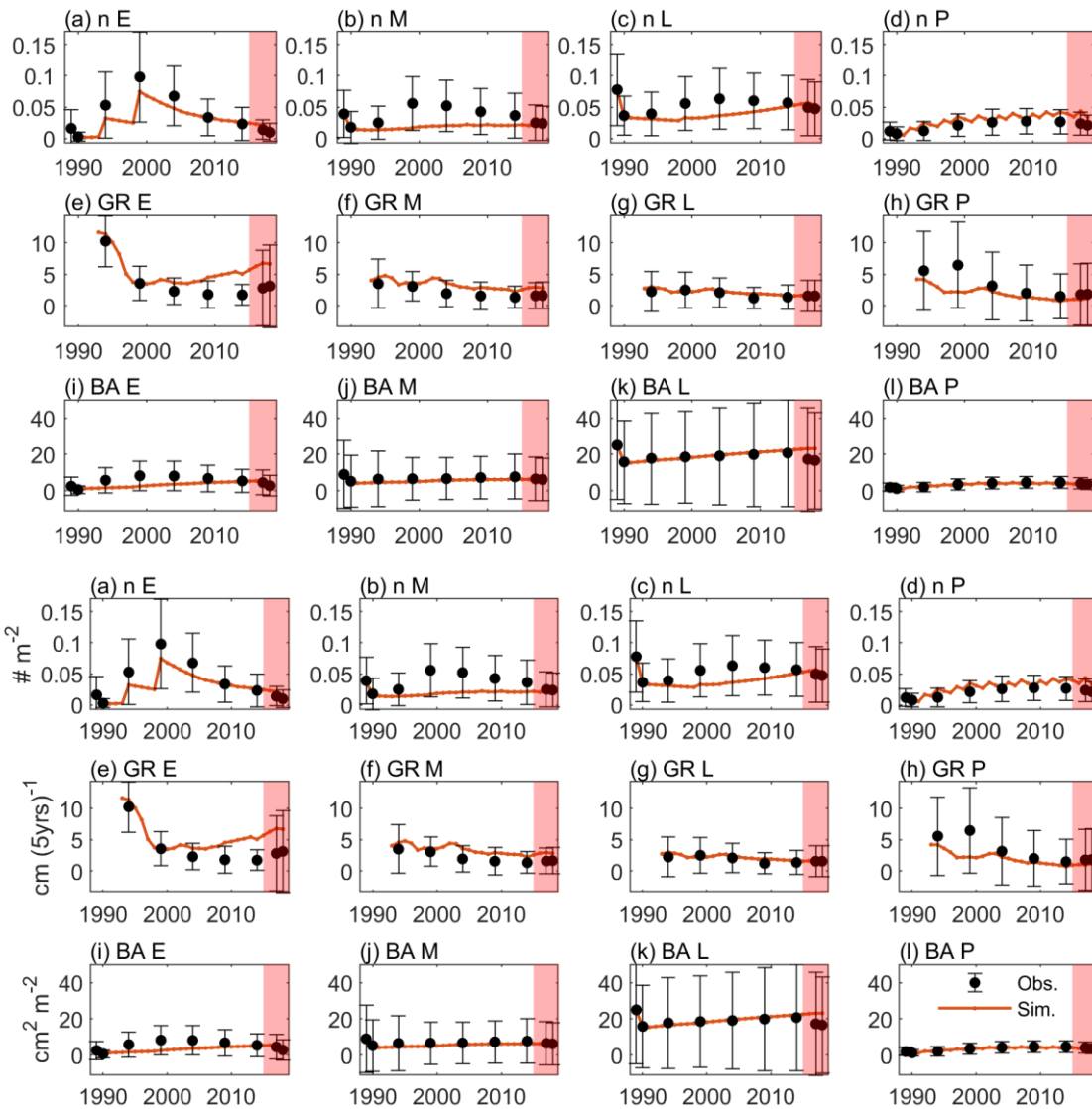
404 To study the impact of the initial condition of the forest on the recovery, we set up two experiments with different
405 initial forest states (pre-Hugo state and pre-Maria state) with a hurricane disturbance in the first simulation year
406 (experiment IhugoH1 and experiment ImariaH1, hereafter), and one control experiment with pre-Hugo state and no
407 hurricane disturbance in all simulation years (experiment IhugoHn, hereafter). The three experiments run for 112
408 simulation years (corresponding to years 1989–2100). The meteorological drivers between 1989 and 2017 are
409 observations from meteorological towers at BEW, and the meteorological drivers between 2018 to 2100 are randomly
410 sampled from the observations between 1989 and 2017. Hurricane disturbance is turned off in all simulation years for
411 experiment IhugoHn and in all but the first simulation year for experiments IhugoH1 and ImariaH1. Thus, experiment
412 IhugoHn represents the succession of the forest without hurricane disturbances for more than a century. Experiments
413 IhugoH1 and ImariaH1 represent the recovery of the forest from a hurricane disturbance given different initial
414 conditions of the forest.

415 3 Results

416 3.1 Model Assessment

417 3.1.1 Optimal Simulation and Optimal Parameter Set

418 Figure 3-4 shows the optimal model simulation along with census observations for years 1989–2018. The simulated
419 stem density of Early increased from 0.0027 individuals m⁻² in 1990 to 0.0324 in 1994 (1100% increase) and to 0.0748
420 in 1999 (131% increase) and decreased steadily thereafter, consistent with observations (0.0030 individuals m⁻² in
421 post-Hugo 1989, 1673% increase in 1994 and 84% increase in 1999). The simulated stem density of Mid is overall
422 underestimated by 47% compared to the mean from the 85 plots of observations, but is within one standard deviation
423 of the observations. The simulated stem density of Late and Palm are also within one standard deviation of the
424 consistent with observations although the mode predictions suggest with 25% underestimation and 38%
425 overestimation, respectively. The optimal simulation overestimates the growth rate of the Early PFT by 133% for
426 years between 2000 and 2014, but it generally captures the decrease of growth rate with time since the hurricane
427 disturbance for all PFTs. Furthermore, the optimal simulation agrees well with the observations for the overall stem
428 density (-21% relative bias), basal area (-12% relative bias), and aboveground biomass (-15% relative bias), and
429 captures well the PFT composition (+1%, -8%, -2%, and +9% differences in the percentages of Early, Mid, Late, and
430 Palm PFTs, respectively) and size structure (+0.8% differences in the percentage of large stems) (Figure 45).

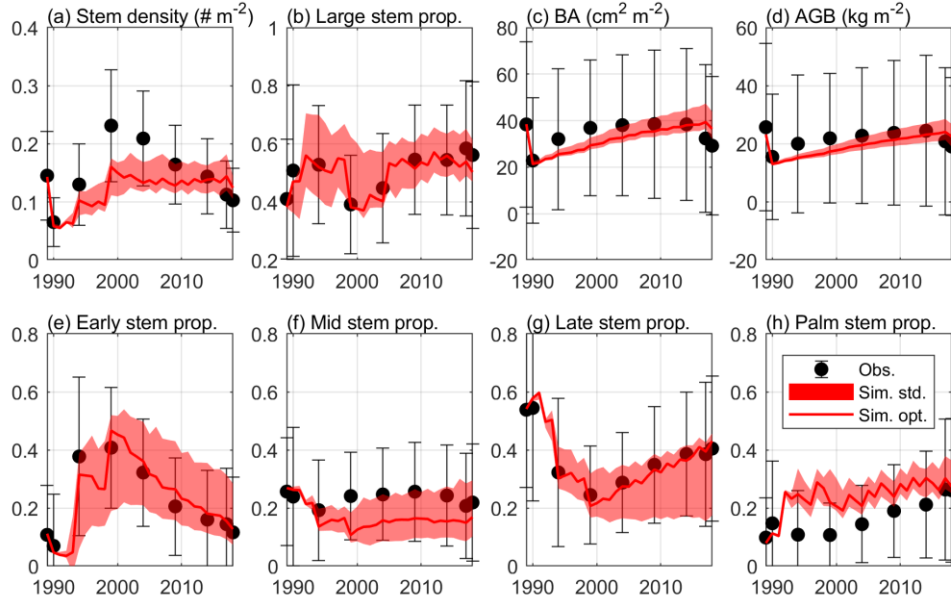


431

432

433 **Figure 43.** Time series of variables from observation (dots and error bars) and the optimal simulation (red lines). (a)-(d) stem
 434 density of all trees (n ; $\text{DBH} \geq 2.5$ cm) (individuals m^{-2}) for Early, Mid, Late, and Palm PFTs, respectively. (e)-(h) diameter growth
 435 rate (GR; $\text{cm} (\text{5yrs})^{-1}$) for the four PFTs; (i)-(l) basal area (BA; $\text{cm}^2 \text{m}^{-2}$) for the four PFTs. The dots and the error bars represent the
 436 means and the one standard deviations from the means across the 85 plots. Period between 1989–2014 is for model calibration and
 437 period between 2015–2018 is for model validation (shaded).

438



439

440 **Figure 54.** The standard deviation of the estimated variables with $K=8$ in equation (4), along with the optimal simulation and
 441 observation. The figure shows (a) stem density of all stems with $DBH \geq 2.5$ cm (individuals m^{-2}), (b) stem density proportion of
 442 large stems with $DBH \geq 10$ cm, (c) basal area (BA; $cm^2 m^{-2}$), (d) aboveground biomass (AGB; $kgC m^{-2}$), and stem density
 443 proportion of (e) Early, (f) Mid, (g) Late, and (h) Palm PFTs.

444

445 In the verification period between 2015–2018, the simulated overall stem density, basal area, and
 446 aboveground biomass have a relative bias of +24%, +23%, and +17%, respectively, ~~compated~~compared to the mean
 447 of the observations. The simulated percentages of the four PFTs have a difference of +3%, -7%, -4%, and 8%,
 448 respectively; and the simulated large stem percentage has a difference of +0.3% compared to the mean of the
 449 observations. Overall, the simulated variables between 2015–2018 are within the standard deviations of the
 450 observations (Figure 3-4 and Figure 45), suggesting that the parameters found using the data between 1989–2014 are
 451 valid for the 2015–2018.

452 Table 1 shows the optimal set of the parameter values. The clumping factor (0.34) is lower than that from
 453 other studies in different locations (~ 0.7 ; He et al. 2012). Other parameters are reasonable and are consistent with
 454 reported values. For example, the leaf turnover rate of Late ($0.16 \text{ year}^{-1}\text{yr}^{-1}$) is consistent with a previous study (~ 0.1 ;
 455 Gill and Jackson 2000). The leaf turnover rate of Palm ($0.42 \text{ year}^{-1}\text{yr}^{-1}$) is consistent with previous observations of
 456 $0.36 \text{ year}^{-1}\text{yr}^{-1}$ at BEW (Lugo et al. 1998). The woody tissue density of Palm (0.24 g cm^{-3}) is consistent with previous
 457 observations of 0.31 g cm^{-3} (Swenson and Umana 2015). ~~0.25 $g cm^{-3}$ for the palm species *Prestoea decurrens* (Zanne~~
 458 ~~et al. 2009; Chave et al. 2009) that is the same genus as the palm species at our study site.~~

459

460 **Table 1.** The optimal parameter set obtained from the GLUE method.

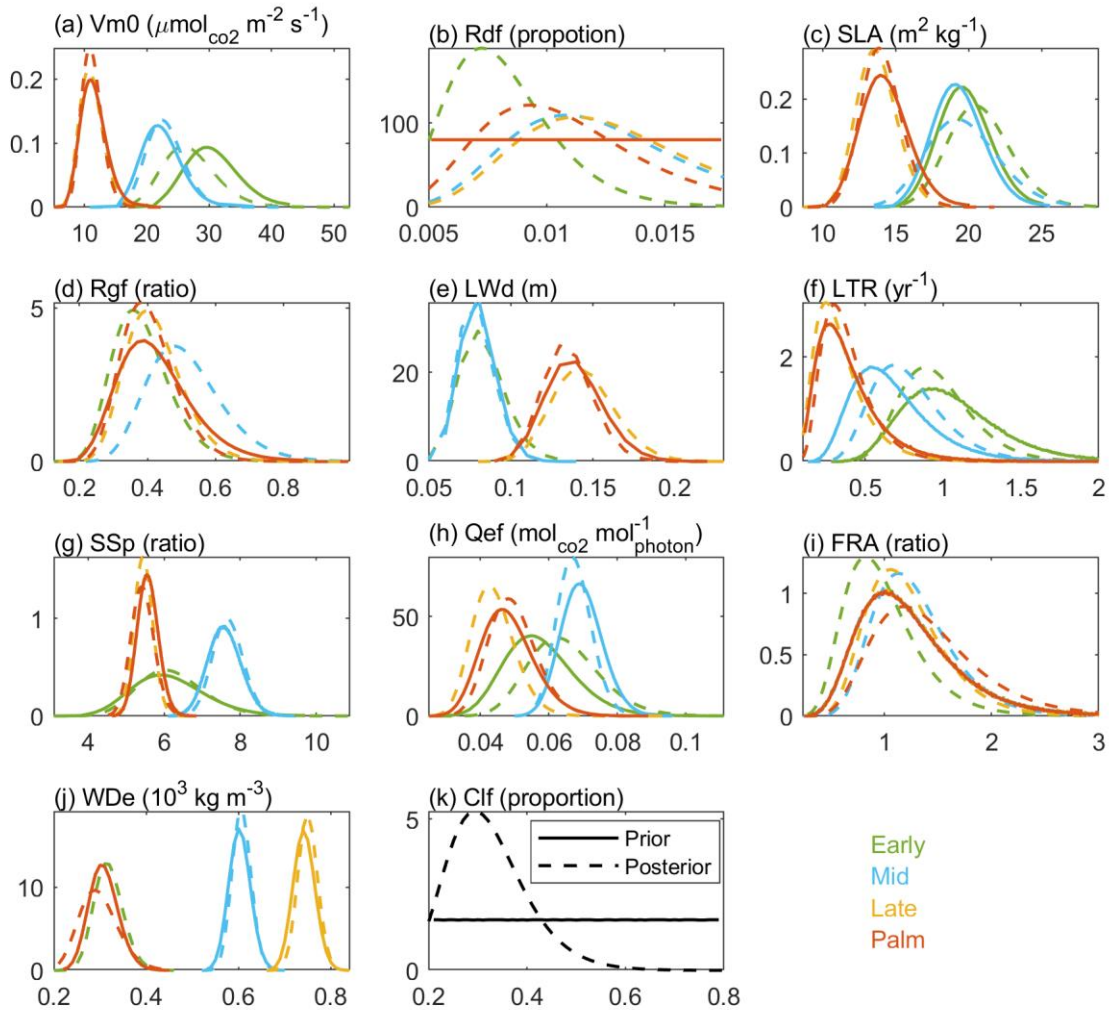
Parameter Name	Units	Early	Mid	Late	Palm
clumping factor (Clf)	proportion	0.34			
fine root allocation (FRA)	ratio	0.64	1.2	0.95	1.85
leaf turnover rate (LTR)	$\text{year}^{-1}\text{yr}^{-1}$	1	0.83	0.16	0.42

leaf width (LWd)	m	0.1	0.07	0.16	0.13
quantum efficiency (Qef)	$\text{mol}_{\text{CO}_2} \text{mol}^{-1}_{\text{photon}}$	0.055	0.069	0.038	0.05
dark respiration rate (Rdf)	proportion	0.0071	0.0144	0.0143	0.0088
growth respiration rate (Rgf)	ratio	0.44	0.595	0.421	0.401
specific leaf area (SLA)	m^2kg^{-1}	23.26	22.28	13.19	14.15
stomatal slope (SSp)	ratio	6.17	8.02	5.35	5.07
carboxylation rate (Vm0)	$\mu\text{mol}_{\text{CO}_2} \text{m}^{-2}\text{s}^{-1}$	23.32	21.73	9.29	12.24
wood density (WDe)	10^3kgm^{-3}	0.32	0.6	0.77	0.24

461

462 3.1.2 Posterior Distribution of Parameters

463 Figure 5–6 shows the posterior and prior probability distribution functions (PDFs) of the parameters. The most
464 significant differences between the posterior and the prior distributions are for the parameters of clumping factor (Clf)
465 and dark respiration rate (Rdf). The posterior PDFs of some parameters (i.e., carboxylation rate, specific leaf area, leaf
466 width, stomatal slope, and wood density), which are well constrained by observational trait data (Feng et al. 2018), do
467 not change much from the priors (the maximum difference between the prior and posterior CDFs is generally less than
468 0.1) ~~because the prior distributions of those parameters are well constrained by observational trait data (Feng et al.~~
469 ~~2018)~~. The posterior PDFs of other parameters (e.g., leaf turnover rate, quantum efficiency, and fine root allocation),
470 especially for the Early and Mid PFTs, with few observational trait data (Feng et al. 2018), changed greatly from the
471 prior distributions (the maximum difference between the distributions is around 0.3).



472

473 **Figure 65.** The prior (solid line) and posterior (dashed line) probability density functions for the four PFTs (colors) of the 11
 474 parameters. The first ten parameters are PFT-dependent, and the last one leaf clumping factor (Clf) is PFT-independent. Palm has
 475 the same prior distribution for all parameters except that the wood density (WDe) of Palm has the same prior distribution
 476 as that of Early. The long name of each parameter is shown in Table 1.

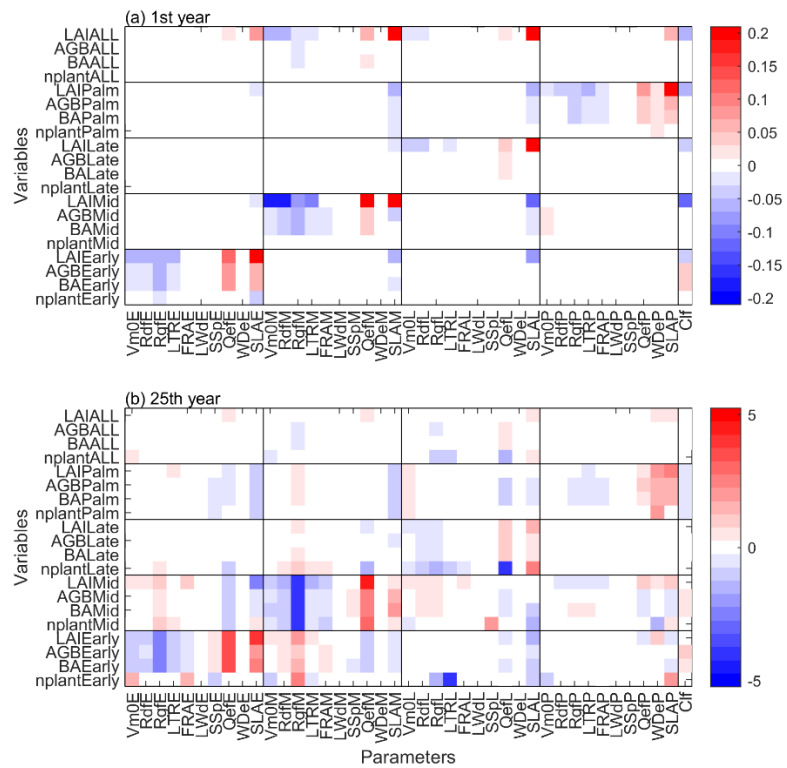
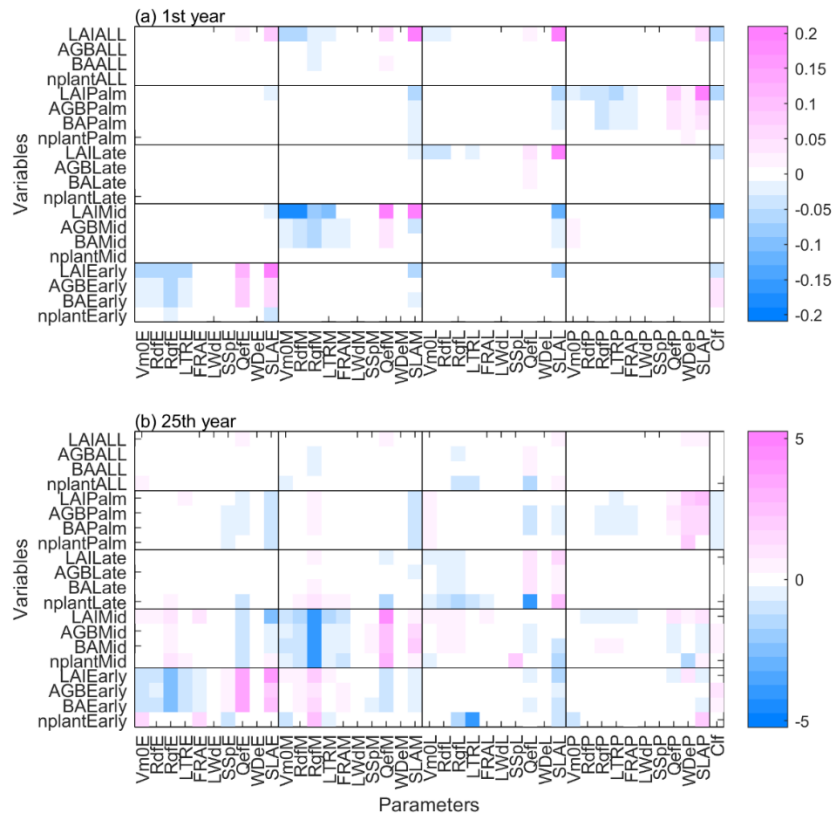
477

478 3.1.3 Parameter Sensitivity and Uncertainty

479 Among the 369 sensitivity experiments with different parameter values, 57 of them have slightly smaller *MSEs* than
 480 the optimal, but the simulated variables (stem density, AGB, PFT composition, and size structure) from those
 481 experiments are very close to those from the optimal (Figure S8S10), indicating that the optimal simulation we found
 482 from GLUE is stable given the uncertainties of the parameters.

483 In terms of the sensitivity-sensitivity of simulated variables on the parameters, the magnitude of standardized
 484 cubic regression coefficients (β) are generally low (~ 0.2) in the first simulation year (Figure 6-7 a), indicating that
 485 the parameters do not have a strong effect on the variables. LAI is the most sensitive variable in the short term, and it
 486 is sensitive to both the specific leaf area (SLA) of its own PFT and the clumping factor (Clf). Furthermore, each PFT

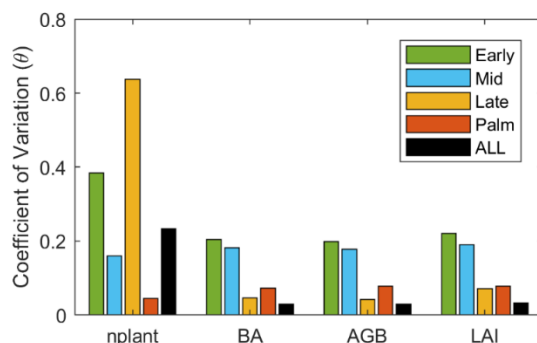
487 is mainly sensitive to the parameters of its own PFT, and vice versa (Figure 6-7 a). After 25 years of simulation, the
488 sensitivity of the variables on the parameters becomes more complex (Figure 6-7 b). First, the magnitude of β increases
489 significantly, indicating that the parameters show stronger impacts on the variables in the long term. Second, the
490 variables are sensitive to different parameters in the short term and in the long term. For example, SLA and clumping
491 factor are the most important parameters to LAI in the first simulation year, but not after 25 years of simulation.
492 Instead, quantum efficiency (Qef) and dark respiration (Rdf) are the most important parameters to LAI after 25 years
493 of simulation. Third, besides the sensitivity of variables to the parameters of their own PFT, variables of a specific
494 PFT also show sensitivity to the parameters of other PFTs. For example, the variables of Early and Mid PFTs are not
495 only sensitive to Early and Mid PFTs parameters, but also sensitive to Late PFT parameters. Specifically, the quantum
496 efficiency, wood density, and specific leaf area have significant positive effects on the variables of its own PFT, but
497 significant negative effects on other PFTs. The Palm PFT is sensitive to its own parameters, but also to the specific
498 leaf area of the Early PFT (Figure 6-7 b).



501 **Figure 76.** The standardized cubic regression coefficient (β) of variables at (a) first and (b) 25th year of the simulations regarding
 502 ~~to~~ the parameters. The variables include stem density (nplant), basal area (BA), aboveground biomass (AGB), and leaf area index
 503 (LAI) for each PFT. The parameters include 10 PFT-dependent parameters and one PFT-~~independent-independent~~ parameter listed
 504 in Table 1.

505

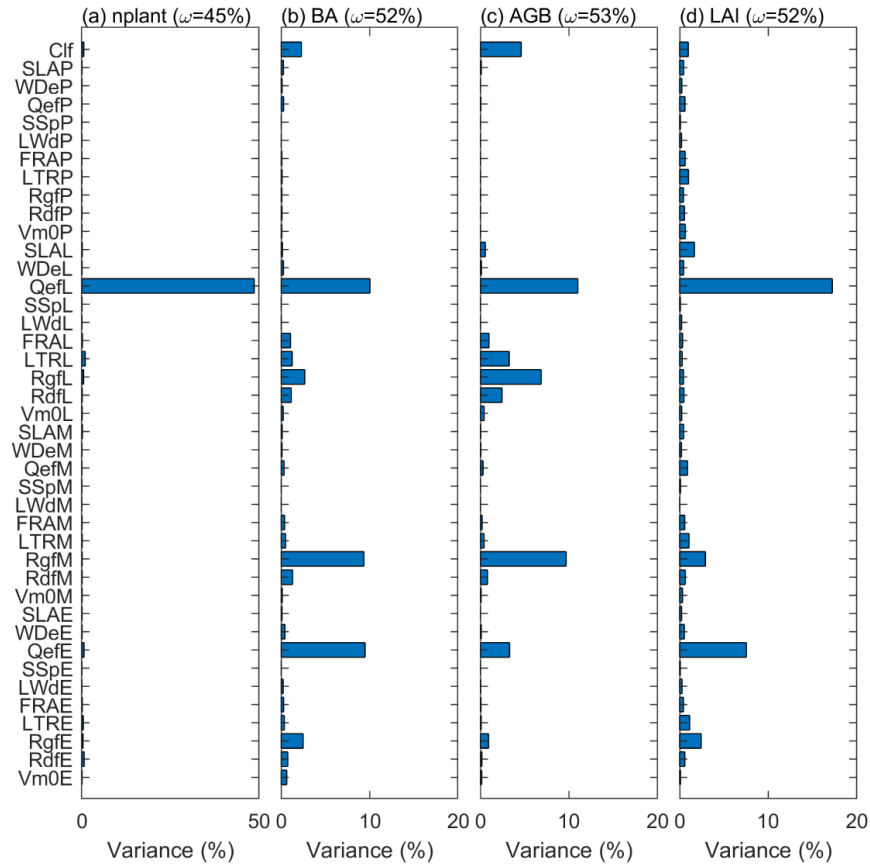
506 The stem density has a larger variation than LAI, BA and AGB after 25 years of simulation (Figure 78).
 507 Given that large stems contribute more to LAI, BA, and AGB, larger variation of stem density than LAI, BA, and
 508 AGB indicates that small stems are more variable than large stems. The variation of those variables also varies with
 509 PFTs. For the stem density, Late PFT has the largest variation, followed by Early, then Mid, and Palm has the smallest
 510 variation, indicating that stem density of small Late is the most sensitive to the uncertainty of the parameters. For BA,
 511 AGB, and LAI, Early and Mid PFTs show the highest variability, followed by the Palm PFT, and the Late PFT has
 512 the lowest variation, indicating that large stems of Early and Mid PFTs are more sensitive to the uncertainty of the
 513 parameters than large stems of Late and Palm PFTs.



514

515 **Figure 87.** The coefficient of variation (θ) for the variables of each PFT at the 25th simulation year.

516



517

518 **Figure 98.** The variance explained by each parameter for variables (a) stem density, (b) basal area, (c) aboveground biomass, and
 519 (d) leaf area index. The variance explained by the interaction among parameters are given in the parenthesis.

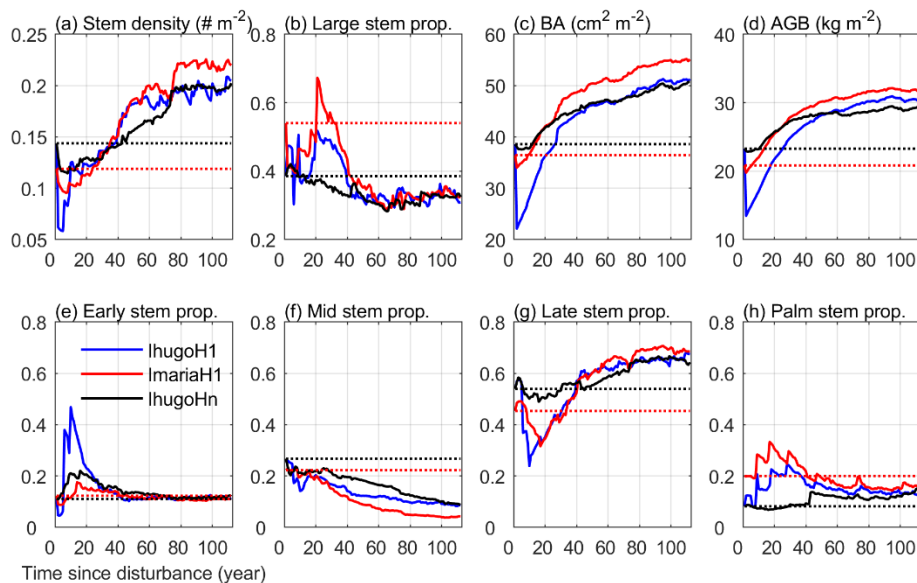
520

521 The variance decomposition analyses reveal that 50% of the uncertainty of the stem density comes from the
 522 quantum efficiency of Late (QefL) (Figure 89). However, QefL explains less than 10% of the uncertainty in BA, AGB,
 523 and LAI, indicating that QefL has significant effects on the density of small stems, but less effects on the density of
 524 large stems. In other words, QefL impacts the recruitment and establishment of stems more than the growth of stems.
 525 The uncertainty of the growth of stems comes from the growth respiration factor (Rgf), which explains about 10% of
 526 the uncertainty. The interaction among parameters accounts for 21% of the uncertainty of the stem density, and more
 527 than 50% of the uncertainty of the BA, AGB, and LAI.

528 3.2 Impact of Initial Condition on Forest Recovery

529 Figure 9-10 shows the 112-year simulations of the forest initialized with different forest states (pre-Maria state and
 530 pre-Hugo state) with or without hurricane disturbance at the first simulation year. Without hurricane disturbance
 531 (IhugoHn), the forest experiences a decrease (-17%) in stem density in the first 10 years due to the self-thinning
 532 process of the forest (Figure 9-10 a). The decrease is mainly attributed to mortality of small stems of Mid and Late
 533 PFTs (Figure 89-91 b and c), which leads to an increase (5%) in the proportion of large stems (DBH ≥ 10 cm) (Figure
 534 9-10 b) but BA and AGB remain steady (Figure 9-10 c and d). After 10 years, a large number of Early PFT stems

535 recruit with DBH less than 10 cm (Figure S9-S11 a), decreasing the overall large stem proportion. After 30 years, Mid
 536 trees recruit and grow (Figure S9-S11 b and Figure S10-S12 b), increasing the total BA and AGB (Figure 9-10 c and
 537 d). As small Late trees recruit frequently after 20 years (Figure S9-S11 c), the stem density increases steadily, and the
 538 proportion of large stems decreases steadily. Because small stems contribute little to BA and AGB, BA and AGB have
 539 a slower increase with time (Figure 9-10 c and d) than stem density (Figure 9-10 a).

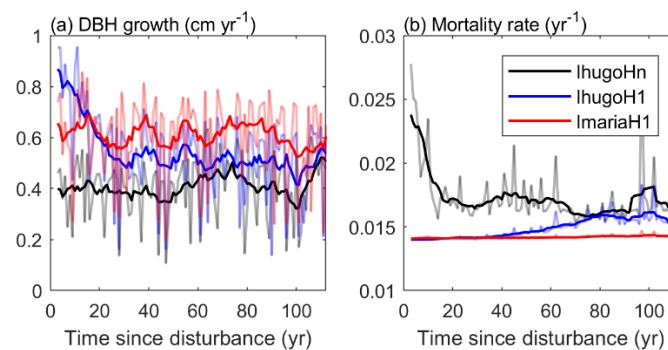


540
 541 **Figure 109.** Time series of eight variables from the simulation of the three experiments: IhugoHn, IhugoH1, ImariaH1. The dotted
 542 lines are the initial state of the variables for each experiment (IhugoHn and IhugoH1 have the same initial state). The variables in
 543 (a) stem density, (c) basal area, and (d) aboveground biomass are for stems with DBH ≥ 2.5 cm. The stem proportion in (b) is the
 544 proportion-proportion of the stem denisty-density with DBH ≥ 10 cm to the stem denisty-density with DBH ≥ 2.5 cm. The variables
 545 in (e)-(h) are the proportion of the stem density of each PFT with DBH ≥ 2.5 cm to the total stem density of all PFTs with DBH \geq
 546 2.5 cm.

547
 548 After 80 years, the PFT composition reaches a steady state (the change of 30-year moving average is less
 549 than 1% compared to the previous year: Figure S13), where the Early, Mid, Late, and Palm PFTs account for 11.8%,
 550 10.6%, 65.3%, and 12.3% of the total stem density, respectively (Figure 9-10 e, f, g, h). This state is significantly
 551 different from the initial state and exhibits a 16% reduction on the proportion of the Mid PFT. It exhibits increases on
 552 all other PFTs proportions (+0.7%, +11.4%, and +4.1% for Early, Late, and Palm, respectively). The Early PFT has
 553 stems of all DBH classes (Figure S9-S11 a); while Mid PFT has mostly small stems with DBH less than 5 cm and a
 554 small cohort (2 individuals ha⁻¹) of large stems with DBH around 200 cm (Figure S11-S14 b and f), which contributes
 555 a significant portion to the total AGB (Figure S10-S12 b). The Late PFT is the most abundant PFT (Figure S9-S11 c)
 556 and contributes the most to the total AGB in the forest (Figure S10-S12 c). The stem density of Late decreases with
 557 DBH (Figure S9-S11 c), and the largest-DBH cohort reaches 180 cm (Figure S11-S14 c), which is smaller than that
 558 of Mid but has a higher density (7 individuals ha⁻¹) (Figure S11-S14 g). The maximum DBH is far larger than that we
 559 observed (89 cm in 2017), but is possible given 100 years of growth with a 2 cm yr⁻¹ increment in DBH (Brandeis
 560 2009)which could be an overestimation due to no nutrient limitation. Palm recruits with DBH between 10 and 15 cm,
 561 the DBH grows slowly after recruitment, and DBH growth stops after they reach the reproduction height (18 m, and

562 25 cm in DBH correspondingly) and allocate all carbon to reproduction (Section 2.2.2-2.1.2), hence palms do not
 563 exceed 25 cm DBH (Figure S11-S14 d) and most of them are between 10 and 20 cm (Figure S9-S11 d and Figure S10
 564 S12 d). This is in agreement with the maximum reported values of DBH (Lugo and Rivera Batlle 1987).

565 Compared with the experiment without hurricane disturbance in the first simulation year (IhugoHn), the ones
 566 experiments with hurricane disturbance in the first simulation year (IhugoH1 and ImariaH1) reach higher BA and
 567 AGB levels after 60 years of succession from the hurricane disturbance (Figure 9-10 c and d). This is due to the carbon
 568 accumulation of large Late PFT in disturbed forests (Figure S10-S12 g and k). Large Late trees in disturbed forest
 569 (IhugoH1 and ImariaH1) have higher growth rate and lower background mortality rate compared to those in the
 570 undisturbed forest (IhugoHn) (Figure 10-11) because of the decreased competition to reach the open canopy. As the
 571 disturbed forest recovers, the BA and AGB increase to the level of the undisturbed forest (Figure 9-10 c and d), the
 572 growth rate decreases (Figure 10-11 a) and the mortality rate increases to the levels of those in the undisturbed forest,
 573 especially for severely disturbed forest (IhugoH1) (Figure 10-11). With lower mortality and higher growth rate in the
 574 first 60 years, there will be more large Late trees in the canopy at the end of the simulation (12 individuals ha⁻¹ vs 8
 575 individuals ha⁻¹) (Figure S11-S14 g) even though the maximum DBH will be smaller (Figure S11-S14 c).



576
 577 **Figure 1140.** Times series of (a) average growth rate and (b) mortality rate of Late trees with DBH ≥ 20 cm. The light-colored
 578 lines represent the yearly values, and the solid lines are ten-year moving averages.

579
 580 The recovery is different with different initial states. With pre-Hugo state (IhugoH1), the forest takes 25 years
 581 to recover to the pre-disturbance BA and AGB levels (Figure 9-10 c and d), but with pre-Maria state (ImariaH1), it
 582 takes only 10 years to recover to the pre-disturbance BA level (Figure 9-10 c) and 5 years to the pre-disturbance AGB
 583 level (Figure 9-10 d). The succession dynamics are different, too. With pre-Hugo state, the hurricane-induced mortality
 584 is very high, and thus the canopy opens, and Early and Palm PFTs recruit greatly in the first 20 years (Figure S9-S11
 585 e and h), and then it is taken over by the Late PFT (Figure S9-S11 g). With pre-Maria initial state, the hurricane-
 586 induced mortality is low, and the canopy is not significantly changed after the hurricane, and Early PFT does not
 587 recruit as much as it does in the pre-Hugo state initialized simulation (Figure S9-S11 i and e). The PFT composition
 588 after 100 years is similar for the two simulations, but the BA and AGB is-are not (Figure 9-10). The BA and AGB with
 589 the pre-Maria initialization are higher than those with the pre-Hugo initialization throughout the 110 years of
 590 simulations, even though the initial AB-BA and AGB levels in the pre-Maria state are lower than those in the pre-
 591 Hugo state (Figure 9-10 c and d). This is because of the higher mortality at the first year with pre-Hugo state, leading
 592 to a larger reduction in the density of large stems. With the succession following the disturbance, there are more large

593 stems, especially Late and Palm, in the pre-Maria simulation than in the pre-Hugo simulation (Figure [S11-S14](#)),
594 contributing to the higher AGB and BA in the pre-Maria simulation (Figure [S10-S12](#) g, h, k, and l).

595 **4 Discussion**

596 We developed a hurricane module (including a mortality module and a recovery module) for the ED2-HuDi model,
597 based on census observations. We then applied a parameter estimation algorithm, GLUE, to calibrate important
598 parameters in the model and selected the optimal parameter set for the final model simulation. However, because the
599 observations are limited to only two hurricane events, the hurricane module may be biased toward the two
600 observations. The simulation results show some discrepancies with observations, and these discrepancies could be in
601 part due to the GLUE approach and parameter uncertainties. Here we discuss the uncertainty associated with the
602 developed hurricane module, the limitations and advantages of the GLUE framework, and the uncertainties of model
603 outputs.

604 **4.1 Uncertainty of the hurricane module**

605 We included a hurricane mortality module and a hurricane recovery module for hurricane disturbance. Crown damage
606 is also an important part of hurricane disturbance and could have important impact on forest structure and carbon
607 accumulation (Leitold et al. 2021), but we did not include crown damage in the hurricane disturbance module because
608 the census data used to develop and calibrate the module do not include crown damage information. The hurricane
609 mortality module was developed based on observations from two hurricane events at the study site. The relationship
610 between mortality and forest size structure (proportion of large stems) was fitted to a logistic function (Figure 2) for
611 each PFT and DBH class. Generally, Palm PFT has a lower mortality than other PFTs, but Palm mortality was higher
612 (11% for Palm, 9% for Mid, and 3% for Late) when the forest was dominated by large stems (e.g., large stem
613 proportion is 0.6, except for the high mortality of 39% for Early (Figure 2b). This was due to the high mortality of
614 Palm during Maria, which was a result of plant pathogens (Zhang et al. 2022b; Heartsill Scalley 2017). The mortality
615 of large-stem Early PFT is significantly different from other PFTs, and this difference was due to the significantly
616 higher mortality of large-stem Early during hurricane Maria compared to other PFTs. Such high mortality of large-
617 stem Early may be a result of other factors besides hurricane disturbance, and it could be further studied if there were
618 more observations. Future work could include observations from other study sites to improve the hurricane disturbance
619 module.

620 There are four critical parameters associated with the hurricane disturbance module, including disturbance
621 rate of forest area (λ_d) and survivorship of each cohort (s_c) from the mortality module, initial seedling density (n_s) and
622 decay factor of seedling density with time since disturbance (α) from the recovery module. We tested the sensitivity
623 of the parameters of the recovery module but did not test the uncertainty of the parameters of the mortality module
624 because the values are from observations at the study site. For future studies using this module, either testing the
625 uncertainty of the parameters or using site specific values are encouraged.

626 **4.1.2 Limitations and Advantages of GLUE**

627 GLUE samples from continuous distributions, but the sampled parameter sets are in a discrete space, therefore, the
628 GLUE approach may not lead to the true optimum due to the finite number of samples. To justify the sample size of
629 10,000 for 41 parameters in this study, we repeated GLUE for a larger sample size (20,000). The optimal simulation
630 from 20,000-sample GLUE (Figure ~~S12~~S15) is very similar to that from the 10,000-sample GLUE (Figure 34) and
631 the optimal parameter sets from the two GLUEs are similar, suggesting that the two GLUEs found an optimum around
632 the same local optimum and 10,000 samples are sufficient for the 41 parameters. However, given the nature of
633 equifinality, there may be multiple parameter sets that can lead to the same observed state (Beven and Freer 2001),
634 and thus the optimal parameter set we found from GLUE may be one of many possible solutions.

635 Although GLUE may not guarantee the global optimum, it ~~implicitly~~ implicitly handles any effects of model
636 nonlinearity, model structure errors, input data errors, and parameters covariation (Beven and Freer 2001). Moreover,
637 GLUE allows us to optimize parameters using any variables of interests in the cost function. For example, in our study,
638 we want to make sure the model captures the size structure and PFT composition of the forest community, and thus
639 we ~~utilized~~ utilized forest stand variables including stem density, growth rate, and BA of each PFT in the cost function.
640 Compared to other optimizers (such as PEcAn) that calibrates parameters using plant traits observations (e.g., wood
641 density, leaf turnover rate), GLUE's ability of ~~utilizing~~ utilizing observations of forest stand variables (BA, AGB, etc.)
642 could further reduce the uncertainty of parameters (Wang et al. 2013). Note that we did not calibrate the parameters
643 using plant traits observations in this study, because the parameters we use are already calibrated with plant traits
644 observations in Feng et al. (2018) and we ~~adpoted~~ adopted their calibrated parameters in our study (see Section 2.3.1-
645 2.3.1).

646 4.24.3 Uncertainty of Model Outputs from Parameters

647 To be consistent with census observations, we included stems with $DBH \geq 2.5$ cm in the analyses. The large
648 variation of simulated stem density (Figure 78) could be due to the timing of cohorts exceeding the 2.5 cm threshold,
649 and thus can be minimized by averaging stem density over several years (Massoud et al. 2019). The optimization is
650 sensitive to light-related parameters, such as clumping factor, quantum efficiency, and dark respiration (Figure 9).
651 This is consistent with Meunier et al. (2021) who found that light limitation contributes partly to model uncertainties.
652 The clumping factor we calibrated for our study site is lower than that from other locations (He et al. 2012), which
653 could be due to uncertainties of the allometries and estimates on the Leaf Area Index (LAI). LAI is generally
654 underestimated in the vegetation dynamics models (e.g., Xu et al. 2016). As discussed in Shiklomanov et al. (2021),
655 the ED2 model has a less robust estimation on LAI because of structural errors in representing direct radiation
656 backscatter. As shown in Figure 6, the clumping factor is one of the most important parameters controlling LAI.
657 However, both LAI and the clumping factor are rarely measured, and LAI estimated from satellite remote sensing
658 data often have variable quality, especially in tropical forests (Xiao et al. 2016, 2017). Future census practices should
659 include LAI and the clumping factor. Even though the LAI measured from the ground may be different from the LAI
660 measured from above the canopy (with airborne lidar or satellites), ground measurements could provide useful
661 information for both the vertical structure of the forest and the quality of satellite remote sensing and airborne lidar
662 data. Furthermore, acclimation to understory light is not considered in this model, however, traits respond strongly to

663 ~~light environments (Lloyd et al. 2010; Keenan and Niinemets 2016), therefore it needs to be considered in future~~
664 ~~developments (Xu and Trugman 2021). The clumping factor we calibrated for our study site is lower than that from~~
665 ~~other locations (He et al. 2012). Observations of clumping factor in our study site are needed to verify the parameter~~
666 ~~from our model calibration and improve model estimates of LAI.~~

667 ~~Our~~ results ~~agree with a previous study~~ that modeled variables have different responses to parameters in
668 the short term (e.g., first simulation year) and in the long term (e.g., 25th simulation year) ~~agree with a previous study~~
669 (Massoud et al. 2019). Furthermore, we showed that variables of a specific PFT are most sensitive to the parameters
670 of the same PFT, but also sensitive to parameters of other PFTs. Those interactions between variables and parameters
671 indicates the competition among PFTs. For example, Palm is sensitive to its own parameters, but also to Early SLA.
672 This can be explained by the competition for light between Early and Palm, where a higher SLA of Early PFT leads
673 to a higher LAI of Early allowing Early to photosynthesize more efficiently and thus be more competitive in the
674 community. Those competitions are important for the co-existence of PFTs in model simulations and critical to the
675 PFT composition and succession.

676 5 Conclusion

677 Hurricanes are a major disturbance to tropical forests, but hurricane disturbance ~~has had~~ not been implemented in any
678 model of vegetation dynamics. In this study, we implemented hurricane disturbance in the Ecosystem Demography
679 model (ED2) and calibrated the model with forest stand observations of a tropical forest in Puerto Rico. The calibrated
680 model has good representation on the recovery trajectory of PFT composition, size structure, stem density, basal area,
681 and aboveground biomass of the forest. We used the calibrated model to study the recovery of the forest from a
682 hurricane disturbance with different initial forest states, and found that a single hurricane disturbance changes forest
683 structure and composition in the short term and enhances AGB and BA in the long term compared with a no-hurricane
684 situation. Forests with wind-resistant initial state will have lower mortality, recover faster, and reach a higher BA and
685 AGB level than forests with a less wind-resistant initial state.

686 The model developed and results presented in this study can be utilized to understand the fate of tropical
687 forests under a changing climate. Hurricanes are likely to become more frequent and severe in the future with global
688 warming (IPCC 2021). With frequent hurricane disturbances in the future, forests will not have enough time to reach
689 a steady state, and the structure and composition will be constantly changing, which provides different initial states
690 for future hurricane disturbances and thus different recovery trajectories. Climate change with changing temperature,
691 precipitation, and CO₂ concentration, etc. will also have an impact on the growth of individual trees and thus the
692 structure and composition of forests (e.g., Feng et al. 2018). The ED2-HuDi model developed in this study will be a
693 beneficial tool to understand the ~~impact-effects~~ of frequent hurricane disturbances on forest recovery in the future
694 under the changing climate.

695
696 *Code and data availability.* The ED2-HuDi software ~~are is~~ publicly available. The most up-to-date source code is
697 available at <https://github.com/zhiyay5/ED2>. The exact version used in this paper is archived on Zenodo

698 (<https://dx.doi.org/10.5281/zenodo.5565063>). Input data and scripts to run the model and produce the plots for all the
699 simulations presented in this paper are also publicly available at <http://www.hydrology.gatech.edu/>.

700
701 *Author contributions.* R.L.B. conceptualized the work, T.H.S. provided field data and contributed ecological
702 ~~perspectives~~[interpretation of the results](#), R.L.B. and J.Z. developed the methodology and performed the analyses, J.Z.
703 and M.L. interpreted results, J.Z. wrote the first draft of the manuscript. All authors discussed results, and critically
704 revised and edited the manuscript.

705
706 *Competing interests.* Authors declare no competing interests.

707
708 *Acknowledgements.* We thank Paul Moorcroft, Xiangtao Xu, Elsa Ordway, Félicien Meunier and Erik Larson for
709 discussions on the model implementation and parameter sensitivity analyses. We acknowledge high-performance
710 computing support from Cheyenne (doi:10.5065/D6RX99HX) provided by NCAR's Computational and Information
711 Systems Laboratory, sponsored by the National Science Foundation. This work was supported by [the](#) National Science
712 Foundation (project EAR1331841) and K. Harrison Brown Family Chair. [This research was supported in part by the](#)
713 [U.S. Department of Agriculture, Forest Service, and the](#) USDA Forest Service International Institute of Tropical
714 Forestry works in collaboration with the University of Puerto Rico. The research was ~~supported by~~ [carried out at](#) the
715 Jet Propulsion Laboratory, California Institute of Technology, under a contract with the National Aeronautics and
716 Space Administration. M.L. was supported by the NASA Postdoctoral Program, administered by Universities Space
717 Research Association under contract with NASA, and by the Next Generation Ecosystem Experiments-Tropics,
718 funded by the U.S. Department of Energy, Office of Science, Office of Biological and Environmental Research. [The](#)
719 [findings and conclusion in this publication are those of the authors and should not be construed to represent any official](#)
720 [USDA or U.S. government policy.](#)

721

722 **References**

- 723 Albani, M, Medvigy, D., Hurtt, G. C., and Moorcroft, P. R.: The ~~contributions~~[contributions](#) of land-use change, CO₂
724 fertilization, and climate variability to the Eastern US carbon sink, *Global Change Biology*, 12, 2370–2390,
725 2006.
- 726 Baraloto, C. et al.: Decoupled lead and stem economics in rain forest trees, *Ecology Letters*, 13, 1338–1347, 2010.
- 727 Beven, K. and Binley, A.: The future of distribution models: Model calibration and uncertainty prediction,
728 *Hydrological Processes*, 6, 279–298, 1992.
- 729 Beven, K. and Freer, J.: Equifinality, data assimilation, and uncertainty estimation in mechanistic modelling of
730 complex environmental systems using the GLUE methodology, *Journal of Hydrology*, 249, 11–29, 2001.
- 731 Binley, A. M. and Beven, K. J.: “Physically-based modelling of catchment hydrology: a likelihood approach to
732 reducing predictive uncertainty”, in: *Computer Modelling in the Environmental Sciences*, edited by: Farmer,
733 D. G. and Rycroft, M. J., Clarendon Press, Oxford, 75–88, 1991.

734 [Boose, E. R., Foster, D. R., and Fluet, M.: Hurricane Impacts of tropical and temperate forest landscapes, Ecological](#)
735 [Monographs, 64, 369–400, 1994.](#)

736 [Boose, E. R., Serrano, M. I., and Foster, D. R.: Landscape and regional impacts of hurricanes in Puerto Rico,](#)
737 [Ecological Monographs, 74, 335–352, 2004.](#)

738 [Brandeis, T. J.: Diameter growth of subtropical trees in Puerto Rico, Res. Pap. SRS 47. Asheville, NC: U.S.](#)
739 [Department of Agriculture Forest Service, Southern Research Station. 39 pp., 2009.](#)

740 Brokaw, N. V. L.: *Cecropia schreberiana* in the Luquillo Mountains of Puerto Rico, Botanical Review, 64, 91–120,
741 <https://www.jstor.org/stable/4354318>, 1998.

742 Chambers, J. Q., Fisher, J. I., Zeng, H., Chapman, E. L., Baker, D. B., and Hurtt, G. C.: Hurricane Katrina's carbon
743 footprint on U.S. Gulf Coast Forests, Science, 318, 1107, 2007.

744 [Chave, J., Coomes, D. A., Jansen, S., Lewis, S. L., Swenson, N. G., and Zanne, A. E.: Towards a worldwide wood](#)
745 [economies spectrum, Ecology Letters, 12, 351–366, 2009.](#)

746 Chen, J. and Black, T.: Foliage area and architecture of plant canopies from sunfleck size distributions, Agricultural
747 and Forestry Meteorology, 60, 249–266, 1992.

748 Cole, L. E. S., Bhagwat, S. A., and Willis, K. J.: Recovery and resilience of tropical forests after disturbance, Nature
749 communications, 5, 3906, 2014.

750 Curran, T. J., Gersbach, L. N., Edwards, W., and Krockenberger, A. K.: Wood density predicts plant damage and
751 vegetative recovery rates caused by cyclone disturbance in tropical rainforest tree species of North
752 Queensland, Australia, Austral Ecology, 33, 442–450, 2008.

753 di Porcia e Brugnera, M. et al.: Modeling the impact of liana infestation on the demography and carbon cycle of
754 tropical forests, Global Change Biology, 25, 3767–3780, 2019.

755 Everham, M. E. III and Brokaw, N. V. L.: Forest damage and recovery from catastrophic wind, The Botanical Review,
756 62, 2, 113–185, 1996.

757 Feng, X. et al.: Improving predictions of tropical forest response to climate change through integration of field studies
758 and ecosystem modeling, Global Change Biology, 24, e213–e232, 2018.

759 Fisher, R. A. and Koven, C. D.: Perspectives on the future of Land Surface Models and the challenges of representing
760 complex terrestrial systems, Journal of Advances in Modeling Earth Systems, 12, e2018MS001453, 2020.

761 Fisher, R. A. et al.: Vegetation demographics in Earth System Models: A review of progress and priorities, Global
762 Change Biology, 24, 35–54, 2018.

763 Francis, J. K. and Gillespie, A. J. R.: Relating gust speed to tree damage in hurricane Hugo, 1989, Journal of
764 Arboriculture, 19, 368–373, 1993.

765 Freer, J., Beven, K., and Ambrose, B.: Bayesian estimation of uncertainty in runoff prediction and the value of data:
766 An application of the GLUE approach, Water Resources Research, 32, 2161–2173, 1996.

767 Gill, R. A. and Jackson, R. B.: Global patterns of root turnover for terrestrial ecosystems, New Phytologist, 147, 13–
768 31, 2000.

769 Gregory, A. A. and Sabat, A. M.: The effect of hurricane disturbance on the fecundity of ~~sierra~~Sierra palms (*Prestoea*
770 *montana*), Bios, 67, 135–139, 1996.

771 Hall, J., Muscarella, R., Quebbeman, A., Arellano, G., Thompson, J., Zimmerman, J. K., and Uriarte, M.: Hurricane-
772 induced rainfall is a stronger predictor of tropical forest damage in Puerto Rico than maximum wind speeds,
773 Scientific Reports, 10, 4318, 2020.

774 He, L., Chen, J. M., Pisek, J., Schaaf, C. B., and Strahler, A. H.: Global clumping index map derived from the MODIS
775 BRDF product, Remote Sensing of Environment, 119, 118–130, 2012.

776 [Heartsill Scalley, T., Scatena, F. N., Lugo, A. E., Moya, S., and Estrada, C. R.: Changes in structure, composition, and](#)
777 [nutrients during 15 years of hurricane-induced succession in a subtropical wet forest in Puerto Rico,](#)
778 [Biotropica, 42, 455–463, 2010.](#)

779 Heartsill Scalley, T.: Insights on forest structure and composition from long-term research in the Luquillo mountains,
780 Forests, 8, 204, 2017.

781 IPCC: Climate Change 2021: The physical science basis. Contribution of Working Group I to the Sixth
782 ~~Assessment~~Assessment Report of the Intergovernmental Panel on Climate Change [Masson-Delmotte, V.
783 et al. (eds.)]. Cambridge ~~Univeristy~~University Press, 2021, In Press.

784 [Jorgensen, S. E.: Overview of the model types available for development of ecological models, Ecological Modelling,](#)
785 [215, 3–9, 2008.](#)

786 [Kammesheidt, L.: Some autecological characteristics of early to late successional tree species in Venezuela, Acta](#)
787 [Oecologica, 21, 37–48, \[https://doi.org/10.1016/S1146-609X\\(00\\)00108-9\]\(https://doi.org/10.1016/S1146-609X\(00\)00108-9\), 2000.](#)

788 [Keenan, T. F., and Niinemets, U.: Global leaf trait estimates biased due to plasticity in the shade, Nature Plants, 3,](#)
789 [16201, 2016.](#)

790 [King, D. A., Davies, S. J., Tan, S., and Noor, N. S. M.: The role of wood density and stem support costs in the growth](#)
791 [and mortality of tropical trees, Journal of Ecology, 94, 670–680, 2006.](#)

792 LeBauer, D. S., Wang, D., Richter, K. T., Davidson, C. C., and Dietze, M. C.: Facilitating feedbacks between field
793 measurements and ecosystem models, Ecological Monographs, 83, 133–154, 2013.

794 Leitold, V. et al.: Tracking the rates and mechanisms of canopy damage and recovery following hurricane Maria using
795 multitemporal Lidar data, Ecosystems, <https://doi.org/10.1007/s10021-021-00688-8>, 2021.

796 Lewis, R. J. and Bannar-Martin, K. H.: The impact of cyclone Fanele on a tropical dry forest in Madagascar,
797 Biotropica, 44, 135–140, 2011.

798 [Lloyd, J. et al.: Optimisation of photosynthetic carbon gain and within-canopy gradients of associated foliar traits for](#)
799 [Amazon Forest trees, Biogeosciences, 7, 1833–1859, 2010.](#)

800 Longo, M. et al.: The biophysics, ecology, and biogeochemistry of functionally diverse, vertically and horizontally
801 heterogeneous ecosystems: the Ecosystem Demography model, version 2.2 – part 1: Model description,
802 Geoscientific Model Development, 12, 4309–4346, 2019a.

803 Longo, M. et al.: The biophysics, ecology, and biogeochemistry of functionally diverse, vertically and horizontally
804 heterogeneous ecosystems: the Ecosystem Demography model, version 2.2 – part 2: Model evaluation for
805 tropical South America, Geoscientific Model Development, 12, 4347–4374, 2019b.

806 Lugo, A. E. and Rivera Batlle, C. T.: Leaf production, growth rate, and age of the palm *Prestoea montana* in the
807 Luquillo Experimental Forest, Puerto Rico, Journal of Tropical Ecology, 3, 151–161, 1987.

808 Lugo, A. E., Francis, J. K., and Frangi, J. L.: *Prestoea montana* (R. Graham) Nichols. Sierra palm. Palmaceae. Palm
809 family, Tech. Rep. SO-ITF-SM-82, US Department of Agriculture, Forest Service, International Institute of
810 Tropical Forestry, 1998.

811 Ma, R.-Y., Zhang, J.-L., Cavaleri, M. A., Sterck, F., Strijk, J. S., and Cao, K.-F.: Convergent evolution towards high
812 net carbon gain efficiency contributes to the shade tolerance of palms (Arecaceae), *PLoS ONE*, 10, e0140384.
813 2015.

814 Massoud, E. C. et al.: Identification of key parameters controlling demographically structured vegetation dynamics in
815 a land surface model: CLM4.5(FATES), *Geoscientific Model Development*, 12, 4133–4164, 2019.

816 [Medlyn, B. E., Robinson, A. P., Clement, R., and McMurtrie, R. E.: On the validation of models of forest CO₂](#)
817 [exchange using eddy covariance data: some perils and pitfalls, *Tree Physiology*, 25, 839–857, 2005.](#)

818 Medvigy, D., Wofsy, S. C., Munger, J. W., Hollinger, D. Y., and Moorcroft, P. R.: Mechanistic scaling of ecosystem
819 function and dynamics in space and time: Ecosystem Demography model version 2, *Journal of Geophysical*
820 *Research*, 114, G01002, 2009.

821 [Medvigy, D., Clark, K. L., Skowronski, N. S., and Schafer, K. V. R.: Simulated impacts of insect defoliation on forest](#)
822 [carbon dynamics, *Environmental Research Letters*, 7, 045703, 2012.](#)

823 [Meunier, F. et al: Unraveling the relative role of light and water competition between lianas and trees in tropical](#)
824 [forests: A vegetation model analysis, *Journal of Ecology*, 109, 519–540, 2021.](#)

825 Meunier, F. et al: Liana optical traits increase tropical forest albedo and reduce ecosystem productivity, *Global Change*
826 *Biology*, [28, 227–244, 2022 in revision.](#)

827 [Miller, A. D., Dietze, M. C., DeLucia, E. H., and Anderson-Teixeira, K. J.: Alteration of forest succession and carbon](#)
828 [cycling under elevated CO₂, *Global Change Biology*, 22, 351–363, 2016.](#)

829 Mirzaei, M., Huang, Y. F., El-Shafie, A., and Shatirah, A.: Application of the generalized likelihood uncertainty
830 estimation (GLUE) approach for assessing uncertainty in hydrological models: A review, *Stochastic*
831 *Environmental Research and Risk Assessment*, 29, 1265–1273, 2015.

832 Moorcroft, P. R., Hurtt, G. C., and Pacala, S. W.: A method for scaling vegetation dynamics: The ecosystem
833 demography model (ED), *Ecological Monographs*, 71, 557–586, 2001.

834 [Muscarella, R. et al.: Life-history trade-offs during the seed-to-seedling transition in a subtropical wet forest](#)
835 [community, *Journal of Ecology*, 101, 171–182, 2013.](#)

836 Muscarella, R. et al.: The global abundance of tree palms, *Global Ecology and Biogeography*, 29, 1495–1514, 2020.

837 Parker, G. et al.: Effects of hurricane disturbance on a tropical dry forest canopy in western Mexico, *Forest Ecology*
838 *and management*, 426, 39–52, 2018.

839 Paz, H., Vega-Ramos, F., and Arreola-Villa, F.: Understanding hurricane resistance and resilience in tropical dry forest
840 trees: A functional traits approach, *Forest Ecology and Management*, 426, 115–122, 2018.

841 Royo, A. A., Heartsill Scalley T., Moya, S., and Scatena, F. N.: Non-arborescent vegetation trajectories following
842 repeated hurricane disturbance: ephemeral versus enduring responses, *Ecosphere*, 27, 77, 2011.

843 Rutledge, B. T., Cannon, J. B., McIntyre, R. K., Holland, A. M., and Jack, S. B.: Tree, stand, and landscape factors
844 contributing to hurricane damage in a coastal plain forest: post-hurricane assessment in a longleaf pine
845 landscape, *Forest Ecology and Management*, 481, 118724, 2021.

846 Sakschewski, B. et al.: Resilience of Amazon forests emerges from plant trait diversity, *Nature Climate Change*, 6,
847 1032–1036, 2016.

848 Scatena, F. N., Silver, W., Siccama, T., Johnson, A., and Sanchez, M. J.: Biomass and nutrient content of the Bisley
849 Experimental Watersheds, Luquillo Experimental Forest, Puerto Rico, before and after hurricane Hugo,
850 1989, *Biotropica*, 25, 15–27, 1993.

851 [Schowalter, T. D., and Ganio, L. M.: Invertebrate communities in a tropical rain forest canopy in Puerto Rico after
852 hurricane Hugo, *Ecol. Entomol.*, 24, 191–201, 1999.](#)

853 [Shiklomanov, A. N., Dietze, M. C., Fer, I, Viskari, T., and Serbin, S. P.: Cutting out the middleman: calibrating and
854 validating a dynamic vegetation model \(ED2-PROSPECT5\) using remotely sensed surface reflectance,
855 *Geosci. Model Dev.*, 14, 2603–2633, 2021.](#)

856 Stein, M.: Large sample properties of simulations using Latin Hypercube sampling, *Technometrics*, 29, 143–151,
857 1987.

858 [Swenson, N. G. and Umana, M. N.: Data from: Interspecific functional convergence and divergence and intraspecific
859 negative density dependence underlie the seed-to-seedling transition in tropical trees, *Dryad, Dataset*,
860 <https://doi.org/10.5061/dryad.j2r53>. 2015.](#)

861 Taylor, J. A. and Lloyd, J.: Sources and Sinks of Atmospheric CO₂, *Australian Journal of Botany*, 40, 407–418, 1992.

862 [Trugman, A. T., Fenton, N. J., Bergeron, Y., Xu, X., Welp, L. R., and Medvigy, D.: Climate, soil organic layer, and
863 nitrogen jointly drive forest development after fire in the North American boreal zone, *Journal of Advances
864 in Modeling Earth Systems*, 8, 1180–1209, 2016.](#)

865 [Uriarte, M., Canham, C. D., Thompson, J., Zimmerman, J. K., and Brokaw, N. Seedling recruitment in a hurricane-
866 driven tropical forest: light limitation, density-dependence and the spatial distribution of parent trees. *Journal
867 of Ecology*, 93, 291–304, 2005.](#)

868 [Uriarte, M. et al.: Natural disturbance and human land use as determinants of tropical forest dynamics: Results from
869 a forest simulator, *Ecological Monographs*, 79, 423–443, 2009.](#)

870 [Uriarte, M, Clark, J. S., Zimmerman, J. K., Comita, L. S., Forero-Montana, J., and Thompson, J.: Multidimensional
871 trade-offs in species responses to disturbance: implications for diversity in a subtropical forest, *Ecology*, 93,
872 191–205, 2012.](#)

873 Uriarte, M., Thompson, J., and Zimmerman, J. K.: Hurricane Maria tripled stem breaks and doubled tree mortality
874 relative to other major storms, *Nature Communications*, 10, 1362, 2019.

875 Walker, L. R.: Tree damage and recovery from hurricane Hugo in Luquillo Experimental Forest, Puerto Rico. Part A.
876 special issue: ecosystem, plant, and animal responses to hurricanes in the Caribbean, *Biotropica*, 23, 379–
877 385, 1991.

878 [Walker, L. R., Voltzow, J., Ackerman, J. D., Fernandez, D. S., and Fetcher, N.: Immediate impact of hurricane Hugo
879 on a Puerto Rico rain forest, *Ecology*, 73, 691–694, 1992.](#)

880 Wang, D., LeBauer, D. and Dietze, M.: Predicting yields of short-rotation hybrid poplar (*Populus* spp.) for the United
881 States through model-data synthesis, *Ecological Applications*, 23, 944–958, 2013.

882 Wang, G. and Eltahir, E. A. B.: Biosphere-atmosphere interactions over West Africa. II: Multiple climate equilibria,
883 *Quarterly Journal of the Royal Meteorological Society*, 126, 1261–1280, 2000.

884 Xiao, Z., Liang, S., Wang, J., Xiang, Y., Zhao X., and Song, J.: Long-time-series global land surface satellite leaf area
885 index product derived from MODIS and AVHRR surface reflectance, *IEEE Transactions on Geoscience and*
886 *Remote Sensing*, 54, 5301–5318, 2016.

887 Xiao, Z., Liang, S., and Jiang, B.: Evaluation of four long time-series global leaf area index products, *Agricultural and*
888 *Forest Meteorology*, 246, 218–230, 2017.

889 Xu, X., Medvigy, D., Powers, J. S., Becknell, J. M., and Guan, K.: Diversity in plant hydraulic traits explains seasonal
890 and inter-annual variations of vegetation dynamics in seasonally dry tropical forests, *New Phytologist*, 212,
891 80–95, 2016.

892 ~~Xu, X., and Trugman, A. T.: trait-based modeling of terrestrial ecosystems: Advances and challenges under global~~
893 ~~change, *Current Climate Change Reports*, 7, 1–13, 2021.~~

894 ~~Zanne, A. E. et al.: Data from: Towards a worldwide wood economics spectrum. *Dryad Digital Repository*.~~
895 ~~<https://doi.org/10.5061/dryad.234>, 2009.~~

896 Zhang, J., Bras, R. L., and Heartsill Scalley, T.: Tree census at Bisley Experimental Watersheds three months after
897 hurricane Maria, Fort Collins, CO: Forest Service Research Data Archive, [https://doi.org/10.2737/RDS-](https://doi.org/10.2737/RDS-2020-0012)
898 [2020-0012](https://doi.org/10.2737/RDS-2020-0012), 2020.

899 Zhang, J., Bras, R. L., and Heartsill Scalley, T.: Tree census at Bisley Experimental Watersheds ~~between 1989 and~~
900 ~~2014. In preparation.~~ ~~before and after Hurricane Hugo, Fort Collins, CO: Forest Service Research Data~~
901 ~~Archive. <https://doi.org/10.2737/RDS-2022-0025>, 2022a.~~

902 Zhang, J., Heartsill Scalley, T., and Bras, R. L.: ~~The importance of forest structure and composition on hurricane~~
903 ~~effects. In revision.~~ ~~Forest structure and composition are critical to hurricane mortality, *Forests*, 13, 202,~~
904 ~~[2022b](https://doi.org/10.2737/RDS-2022-0025).~~

905 ~~Zhang, J., Heartsill Scalley, T., and Bras, R. L.: Parsing long-term tree recruitment, growth, and mortality to identify~~
906 ~~hurricane Hugo's effects on the Luquillo Experimental Forest in Puerto Rico. In revision.~~

907 ~~Zhang, K. et al.: The fate of Amazonian ecosystems over the coming century arising from changes in climate,~~
908 ~~atmospheric CO₂ and land-use, *Global Change Biology*, 21, 2569–2587, 2015.~~

909 Zimmerman, J, K. et al.: Responses of tree species to hurricane winds in subtropical wet forest in Puerto Rico:
910 Implications for tropical tree life histories, *Journal of Ecology*, 82, 911–922, 1994.

911